

博士學位論文



濟州大學校 大學院

通信工學科

李 權 益

2004年 12月

指導教授 金 興 洙
李 權 益

論文 工學 博士學位 論文 提出

2004年 12月

李權益 工學 博士學位 論文 認定



제주대학교 중앙도서관
JEJU NATIONAL UNIVERSITY LIBRARY

審查委員長 梁 斗 榮

委 員 康 鎮 植

委 員 姜 致 雲

委 員 柳 晃

委 員 金 興 洙

濟州大學校 大學院

2004年 12月

Design and fabrication of the cylindrical dielectric resonator antenna with dielectric clad

Kwoun - Ig Lee
(Supervised by professor Heung - Soo Kim)

A thesis submitted in partial fulfillment of the requirement for the degree of
Doctor of Engineering

2004. 12. .

This thesis has been examined and approved.

Thesis director, Doo - Yeong Yang, Prof. of Telecommunication Eng.



Thesis director, Jin - Shig Kang, Prof. of Telecommunication Eng.



Thesis director, Chi - Woon Kang, Prof. of Information & Comm. Eng.



Thesis director, Hwang Ryu, Prof. of Information & Communication



Thesis director, Heung - Soo Kim, Prof. of Telecommunication Eng.



(Name and signature)

2004.12.

Date

Department of Telecommunication Engineering
GRADUATE SCHOOL
CHEJU NATIONAL UNIVERSITY

.....	i
.....	iv
.....	v
.....	ix
Abstract	1
I.	3
II.	6
1.	6
2.	8
3.	18
1)	19
2) 가	20
3) Far - field	23
4. CDRA	28
1)	28
2)	31
3)	34



4)	(loop)	35
III.		38
1.		38
2.		44
1)	DRA	44
2)	DRA	49
3.		51
IV.		55
1.	CDRA	55
2.		57
1)	CDRA	58
2)	<i>b/a</i>	67
3)		70
4)	CDRA	73
5)	CDRA	78
V.		80
1.		80
2.		83
1)		83
2)		85



..... 89

..... 91



Table 1. Minimum bandwidth for each relative permittivity	44
Table 2. Values of x_{11} for various ratios for a/b	47
Table 3. Effect of a/b on the resonant frequency and bandwidth of annular DRA.....	48
Table 4. Design parameters of a CDRA.....	55
Table 5. Resonant frequency and bandwidth of equivalent model($\epsilon_{r2} = 4$)	60
Table 6. Frequency response for each CDRA by eq. (53)	60
Table 7. Frequency response for each CDRA by a simulation tool.....	61
Table 8. Comparison for each CDRA model($b/a=1.3$)	65
Table 9. Design parameters of equivalent model with $b/a = 1.3$	65
Table 10. Bandwidth and resonant frequency of CDRA with the dielectric clad according to b/a	68
Table 11. Resonant frequency and bandwidth according to ϵ_{r2} of dielectric clad	71
Table 12. Frequency response for each CDRA.....	74
Table 13. Design parameters of CDRA with dielectric clad.....	75
Table 14. Fabricated parameters of CDRA	80
Table 15. Fabricated parameters of CDRA with dielectric clad.....	80
Table 16. Resonant frequency and relative bandwidth for each models.....	85

Fig. 1. Cylindrical dielectric waveguide model.....	6
Fig. 2. The eigenvalues of cylindrical dielectric waveguide($\epsilon_r = 10$)	16
Fig. 3. Cylindrical dielectric waveguide mode patterns	17
Fig. 4. Geometry of a CDRA	18
Fig. 5. Feed configuration of a CDRA.....	19
Fig. 6. Calculated radiation patterns of CDRA	25
Fig. 7. Sketch for the field distributions of cylindrical dielectric waveguide.....	26
Fig. 8. Ideal radiation patterns for the $TM_{01\delta}$ mode above infinite ground plane	27
Fig. 9. Ideal radiation patterns for the $HEM_{11\delta}$ mode above infinite ground plane.....	27
Fig. 10. Geometry of aperture - coupled CDRA	28
Fig. 11. Equivalent model of aperture - coupled CDRA	29
Fig. 12. The field distribution of aperture - fed CDRA.....	30
Fig. 13. Geometry of Coaxial probe - fed CDRA	31

Fig. 14. Equivalent model of coaxial probe - fed CDRA	32
Fig. 15. The field distribution of a probe - fed CDRA	33
Fig. 16. Geometry of Microstrip line fed CDRA	34
Fig. 17. Equivalent model of microstrip line fed CDRA	34
Fig. 18. Geometry of co - planar loop - fed CDRA	35
Fig. 19. Equivalent model of co - planar loop - fed CDRA	36
Fig. 20. Geometry of Co - planar slot - fed CDRA	36
Fig. 21. Equivalent of Co - planar slot - fed CDRA	37
Fig. 22. The CDRA mounted on a ground plane	38
Fig. 23. Relative bandwidth of CDKAs with $\epsilon_r = 10$	40
Fig. 24. Resonant frequency for the $TM_{01\delta}$ mode of CDRA	41
Fig. 25. Radiation Q - factor for the $TM_{01\delta}$ mode of CDRA	42
Fig. 26. Relative bandwidth for the $TM_{01\delta}$ mode of CDRA	43
Fig. 27. Geometry of the annular DRA	45
Fig. 28. Equivalent model of the annular DRA	45
Fig. 29. Solution of x_{11} for values of a/b	47
Fig. 30. Return loss of annular DRA according to a/b	48

Fig. 31. The field distribution for the annular DRA	50
Fig. 32. The radiation patterns for the annular DRA	50
Fig. 33. Lumped element impedance model for a two - DRA configuration.....	51
Fig. 34. Dual band and broadband response for a two - DRA configuration	53
Fig. 35. Annular DRA with embedded CDRA	54
Fig. 36. Top views of annular DRA with embedded CDRA.....	54
Fig. 37. Geometry of a probe - fed CDRA	55
Fig. 38. The return loss of CDRA	56
Fig. 39. Input impedance of a CDRA according to probe length	57
Fig. 40. Geometry of a CDRA with a dielectric clad	58
Fig. 41. Geometry and equivalent model of CDRA with dielectric clad.....	59
Fig. 42. Return loss of equivalent model with according to b/a ratio.....	62
Fig. 43. Return loss of each CDRA ($b/a = 1.2$)	63
Fig. 44. Return loss of each CDRA ($b/a = 1.3$).....	64
Fig. 45. Return loss of equivalent model with $b/a = 1.3$	66
Fig. 46. Return loss of each CDRA	67
Fig. 47. Behavior of return loss with b/a as parameter.....	68

Fig. 48. Bandwidth and resonant frequency with b/a as parameter	69
Fig. 49. Radiation patterns according to b/a	70
Fig. 50. Return loss of CDRA according to the relative permittivities of dielectric clad	71
Fig. 51. Relative bandwidth according to the relative permittivities of dielectric clad	72
Fig. 52. Radiation patterns according to the relative permittivities of dielectric clad	73
Fig. 53. Return loss of CDRA according to modified relative permittivities	74
Fig. 54. Return loss for three CDRA models	76
Fig. 55. Field distribution of the CDRA with dielectric clad	77
Fig. 56. Flow chart for design procedure	78
Fig. 57. Photos of coaxial probe feed	81
Fig. 58. Photo of the fabricated CDRA	82
Fig. 59. Photo of the fabricated CDRA with dielectric clad	83
Fig. 60. Measured return loss of CDRA	84
Fig. 61. Measured radiation patterns of CDRA	84

Fig. 62. Return loss of CDRA and CDRA with dielectric clad85

Fig. 63. Gain of the fabricated CDRA with dielectric clad.....86

Fig. 64. Return loss of the fabricated CDRA with dielectric clad87

Fig. 65. Measured radiation patterns of CDRA with dielectric clad87



ϵ 1

ϵ_{r1} 1

ϵ_{r2}	2
$\epsilon_{r\text{mod}}$	
μ	
k_0	
k	
J_m	m 1
Y_m	m 2
K_m	m 2
x_{mn}	
k_0a	
f_0	
Q factor	Q
S	VSWR
BW	
f_u	
f_l	
Δf_u	f_u
Δf_l	f_l
DR	
DRA	
CDRA	
RDRA	



CPW



Abstract

Because the compact and broadband services are recently demanded in radio communication system, the antennas that have compactness and broadband characteristics are required. Dielectric resonator antennas, as compared with the microstrip antenna, have high radiation efficiencies because of low resistance loss and have broadband characteristics. Due to their resonance nature, dielectric resonator antennas have a limited bandwidth, so the new type of dielectric resonator antenna which can expand bandwidth is required.

In this thesis, a new type of dielectric resonator antenna, which can improve the limited bandwidth of cylindrical dielectric resonator antenna, and the design method of this antenna are proposed. The resonant frequency and the bandwidth of cylindrical dielectric resonator antenna are calculated from eigenvalue to each mode of cylindrical dielectric waveguide. In order to analyze frequency characteristics of the proposed antenna, an equivalent dielectric model, which is composed of relative permittivity of inner cylindrical dielectric resonator antenna and relative permittivity of dielectric clad, is proposed. By using this model, the resonant frequency and the bandwidth are calculated and frequency - response characteristics of cylindrical dielectric resonator antenna and equivalent model are synthesized. Broadband frequency - response is determined with respect to the change of aspect ratio and relative permittivity of dielectric clad. When an aspect ratio(a/b) is more than 1.3 and relative permittivity is below 1/2, the broadband response of proposed antenna is obtained. Design parameters of dielectric clad that has maximum bandwidth under this condition are obtained by HFSS which is three dimensional finite element method (FEM) simulation tools. In the case of the aspect ratio is increased

and relative permittivity is decreased, resonant frequency is become low, but not affected on the radiation pattern and gain. Specially, Compared with cylindrical dielectric resonator antenna, the bandwidth of proposed antenna is improved about 40% when the aspect ratio is 1.4 and relative permittivity of dielectric clad is one - third of the cylindrical dielectric resonator antenna. On the basis of these procedures, the design method of cylindrical dielectric resonator antenna with dielectric clad is proposed. In order to verify the validity of design method, the parameters of proposed antenna are selected as relative permittivity of cylindrical dielectric resonator $\epsilon_{r1} = 10$, radius $a = 10.65$ mm, the aspect ratio of $b/a = 1.44$ and relative permittivity of dielectric clad $\epsilon_{r2} = 4$, and compared with simulated results. The resonant frequency and the relative bandwidth are obtained 5.68GHz and 22.2% by simulated antenna, and 5.91GHz and 28.8% by fabricated one. Error ranges of resonant frequency and relative bandwidth, which are measured and simulated, are within 4% and the validity of design method is verified.



I.

(DR; dielectric resonator)

($\epsilon_r > 20$)

(Q:quality factor)

DR

DR Long (1983)

(CDRA; cylindrical dielectric resonator antenna)

가

(DRA; dielectric

resonator antenna)

. CDRA가



제주대학교 중앙도서관
Long (1983) UNIVERSITY LIBRARY

Mongia

Ittipiboon(1997)

, Kishk Glisson(2001)

Lo

(2000)

DRA

(Petosa 1998).

DRA

가

. DRA Junker (1995),

Shum Luk(1995)

, Lee (1999), Leung (1997)

, Antar (1990), Kishk (1985), Leung (1998)

Karanenburg (1990) CPW(Co - Planar

Waveguide)

(Ong 2002). (Chow 1997),
 Q Mongia (1993)
 Shum Luk(1994a, 1994b), Junker (1994)
 Q
 Q 가
 가 가
 가 DRA
 (Leung 1996), (Luk Shum, 1994),
 (Sangiovanni 1997), (Kajfez 1989), (, 2003).

(Nannini 2004).
 제주대학교 중앙도서관
 (Shum Luk, 1995), (Kajfez 1989), (Junker 1995).
 SEJU NATIONAL UNIVERSITY LIBRARY

1/2

(Kishk Glisson, 2001), (Chen Wong, 1995).

CDRA

CDRA

CDRA

CDRA

DRA CDRA가

DRA

CDRA

가

CDRA

CDRA

CDRA

CDRA

CDRA



제주대학교 중앙도서관
JEJU NATIONAL UNIVERSITY LIBRARY

CDRA

가

가

CDRA

VI

II.

CDRA 가 ,
 DRA 가 .
 $TM_{01\delta}$
 CDRA CDRA

1.



Fig. 1

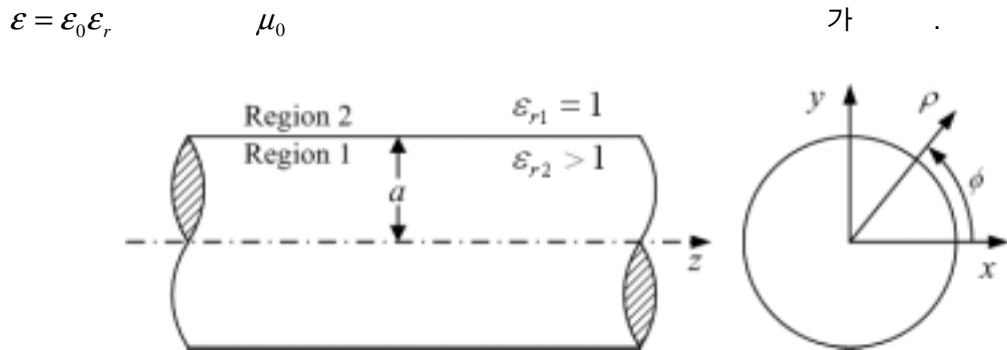


Fig. 1. Cylindrical dielectric waveguide model

$$\rho \frac{1}{P} \frac{d}{d\rho} \left(\rho \frac{d}{d\rho} P \right) + \frac{1}{F} \frac{d^2 F}{d\phi^2} + (k^2 - \beta^2) \rho^2 = 0 \quad (5)$$

$$(5) \quad \phi \quad \rho$$

$$\frac{1}{F} \frac{d^2 F}{d\phi^2} = -m^2 \quad (6)$$

$$m \quad (6) \quad (5) \quad P$$

$$\rho \frac{d}{d\rho} \left(\rho \frac{d}{d\rho} P \right) + [(k_\rho \rho)^2 - m^2] P = 0 \quad (7)$$

$$k_\rho^2 = k^2 - \beta^2$$

$$(4) \quad (6) \quad (\text{harmonic}) \quad (7) \quad m \quad (\text{Bessel})$$

$$(4) \quad \beta \quad m \quad (4), (6) \quad (7)$$

가 (Kajfez

Guillon, 1986).

2.

$$E_z \quad H_z \quad \phi \quad 2\pi$$

z 가 .

$E_z \quad H_z$

$$E_{z1} = AJ_m(k_{\rho1}\rho) \begin{bmatrix} \cos(m\phi) \\ \sin(m\phi) \end{bmatrix} e^{-j\beta z} \quad (8a)$$

$$H_{z1} = BJ_m(k_{\rho1}\rho) \begin{bmatrix} \sin(m\phi) \\ \cos(m\phi) \end{bmatrix} e^{-j\beta z} \quad (8b)$$

m , J_m 1 m Bessel .

$$k_{\rho1}^2 = k^2 - \beta^2 \quad (9)$$

$$(9) \quad k = k_0 \sqrt{\epsilon_r} \quad , \quad k_0$$



제주대학교 중앙도서관
JEJU NATIONAL UNIVERSITY LIBRARY

가

$$E_{z2} = CK_m(k_{\rho2}\rho) \begin{bmatrix} \cos(m\phi) \\ \sin(m\phi) \end{bmatrix} e^{-j\beta z} \quad (10a)$$

$$H_{z2} = DK_m(k_{\rho2}\rho) \begin{bmatrix} \sin(m\phi) \\ \cos(m\phi) \end{bmatrix} e^{-j\beta z} \quad (10b)$$

K_m 2 m Bessel .

$$k_{\rho2}^2 = \beta^2 - k_0^2 \quad (11)$$

E_z	H_z	$0 < \phi < 2\pi$		E_z	H_z
cosine	sine		$m = 0$	ϕ	
z		(TE)	(TM)		
	$m > 0$	TE	TM		
(HEM)					

$$H_{\rho 1} = \frac{1}{k_{\rho 1}^2} \left[-j\omega\epsilon_0 m \frac{A}{\rho} J_m(k_{\rho 1}\rho) - j\beta k_{\rho 1} B J_m'(k_{\rho 1}\rho) \right] \sin(m\phi) e^{-j\beta z} \quad (12a)$$

$$E_{\phi 1} = \frac{1}{k_{\rho 1}^2} \left[j\beta m \frac{A}{\rho} J_m(k_{\rho 1}\rho) + j\omega\mu_0 k_{\rho 1} B J_m'(k_{\rho 1}\rho) \right] \sin(m\phi) e^{-j\beta z} \quad (12b)$$

$$E_{\rho 1} = \frac{1}{k_{\rho 1}^2} \left[-j\beta k_{\rho 1} A J_m'(k_{\rho 1}\rho) - j\omega\mu_0 m \frac{B}{\rho} J_m(k_{\rho 1}\rho) \right] \cos(m\phi) e^{-j\beta z} \quad (12c)$$

$$H_{\phi 1} = \frac{1}{k_{\rho 1}^2} \left[-j\omega\epsilon_0 k_{\rho 1} A J_m'(k_{\rho 1}\rho) - j\beta m \frac{B}{\rho} J_m(k_{\rho 1}\rho) \right] \cos(m\phi) e^{-j\beta z} \quad (12d)$$

$$H_{\rho 2} = \frac{-1}{k_{\rho 2}^2} \left[-j\omega\epsilon_0 m \frac{C}{\rho} K_m(k_{\rho 2}\rho) - j\beta k_{\rho 2} D K_m'(k_{\rho 2}\rho) \right] \sin(m\phi) e^{-j\beta z} \quad (13a)$$

$$E_{\phi 2} = \frac{-1}{k_{\rho 2}^2} \left[j\beta m \frac{C}{\rho} K_m(k_{\rho 2}\rho) + j\omega\mu_0 k_{\rho 2} D K_m'(k_{\rho 2}\rho) \right] \sin(m\phi) e^{-j\beta z} \quad (13b)$$

$$E_{\rho 2} = \frac{-1}{k_{\rho 2}^2} \left[-j\beta k_{\rho 2} C K_m'(k_{\rho 2}\rho) - j\omega\mu_0 m \frac{D}{\rho} K_m(k_{\rho 2}\rho) \right] \cos(m\phi) e^{-j\beta z} \quad (13c)$$

$$H_{\phi 2} = \frac{-1}{k_{\rho 2}^2} \left[-j\omega\epsilon_0 k_{\rho 2} CK_m'(k_{\rho 2}\rho) - j\beta m \frac{D}{\rho} K_m(k_{\rho 2}\rho) \right] \cos(m\phi) e^{-j\beta z} \quad (13d)$$

$$E_{z1} = E_{z2} \quad (14a)$$

$$H_{z1} = H_{z2} \quad (14a)$$

$$E_{\phi 1} = E_{\phi 2} \quad (14a)$$

$$H_{\phi 1} = H_{\phi 2} \quad (14a)$$

$$(12) \quad (13) \quad \rho = a \quad , \quad (14)$$



$$AJ_m(k_{\rho 1}a) - CK_m(k_{\rho 2}a) = 0 \quad (15a)$$

$$BJ_m(k_{\rho 1}a) - DK_m(k_{\rho 2}a) = 0 \quad (15b)$$

$$\begin{aligned} & \frac{\beta}{k_{\rho 1}^2 a} mAJ_m(k_{\rho 1}a) + \frac{\omega\mu_0}{k_{\rho 1}} BJ_m'(k_{\rho 1}a) \\ & + \frac{\beta}{k_{\rho 2}^2 a} mCK_m(k_{\rho 2}a) + \frac{\omega\mu_0}{k_{\rho 2}} DK_m'(k_{\rho 2}a) = 0 \end{aligned} \quad (15c)$$

$$\begin{aligned} & \frac{\omega\epsilon}{k_{\rho 1}^2 a} AJ_m'(k_{\rho 1}a) + \frac{\beta}{k_{\rho 1}^2 a} BJ_m(k_{\rho 1}a) \\ & + \frac{\omega\epsilon_0}{k_{\rho 2}} CK_m'(k_{\rho 2}a) + \frac{\beta}{k_{\rho 2}^2 a} mDK_m(k_{\rho 2}a) = 0 \end{aligned} \quad (15d)$$

$$(15)$$

$$x = k_{\rho 1} a \quad (16a)$$

$$y = k_{\rho 2} = \sqrt{(k_0 a)^2 (\varepsilon_r - 1) - x^2} \quad (16b)$$

$$\beta a = \sqrt{(k_0 a)^2 \varepsilon_r - x^2} \quad (16c)$$

(16)

(15)

$$AJ_m(x) - CK_m(y) = 0 \quad (17a)$$

$$BJ_m(x) - DK_m(y) = 0 \quad (17b)$$

$$\begin{aligned} \frac{\beta a m}{x^2} AJ_m(x) + \frac{\omega \mu_0 a}{x} BJ_m'(x) \\ + \frac{\beta a m}{y^2} CK_m(y) + \frac{\omega \mu_0 a}{y} DK_m'(y) = 0 \end{aligned} \quad (17c)$$

$$\begin{aligned} \frac{\omega \varepsilon a}{x} AJ_m'(x) + \frac{\beta a m}{x^2} BJ_m(x) \\ + \frac{\omega \varepsilon_0 a}{y} CK_m'(y) + \frac{\beta a m}{y^2} DK_m(y) = 0 \end{aligned} \quad (17d)$$

(17)

$$[F][U]=0 \quad (18)$$

$$[F] \quad (19) \quad 4 \times 4 \quad .$$

$$F = \begin{bmatrix} J_m(x) & 0 & -K_m(y) & 0 \\ 0 & J_m(x) & 0 & -K_m(y) \\ \frac{\beta am}{x^2} J_m(x) & \frac{\omega \mu_0 a}{x} J_m'(x) & \frac{\beta am}{y^2} K_m(y) & \frac{\omega \mu_0 a}{y} K_m'(y) \\ \frac{\omega \epsilon a}{x} J_m'(x) & \frac{\beta am}{x^2} J_m(x) & \frac{\omega \epsilon_0 a}{y} K_m'(y) & \frac{\beta am}{y^2} K_m(y) \end{bmatrix} \quad (19)$$

$$U \quad \text{가 } A, B, C, D \quad 4 \times 1 \quad .$$

$$U = \begin{bmatrix} A \\ B \\ C \\ D \end{bmatrix} \quad (20)$$



$$(19) \quad \text{non-trivial} \quad x \text{가} \quad .$$

$$\det(F)=0 \quad (21)$$

$$(21) \quad .$$

$$\begin{aligned}
& \frac{\omega\epsilon a}{x} J_m'(x)K_m(y) \left[\frac{\omega\mu_0 a}{y} J_m(x)K_m'(y) + \frac{\omega\mu_0 a}{x} K_m(y)J_m'(x) \right] \\
& - \frac{\beta am}{x^2} J_m(x)K_m(y) \left[\frac{\beta am}{y^2} J_m(x)K_m(y) + \frac{\beta am}{x^2} J_m(x)K_m(y) \right] \\
& + J_m^2(x) \left[-\frac{(\beta am)^2}{y^4} K_m^2(y) + \frac{\omega\mu_0^2 \epsilon_0 a^2}{y^2} K_m'^2(y) \right] \\
& + J_m(x)K_m(y) \left[\frac{\omega\mu_0 \epsilon_0^2 a}{xy} J_m'^2(x)K_m'(y) - \frac{(\beta am)^2}{x^2 y^2} J_m(x)K_m(y) \right] = 0
\end{aligned} \tag{22}$$

$$(22) \quad (K_m^2(y)/\omega^2 \mu_0 \epsilon a^2)$$

$$F_1(x)F_2(x) - F_3^2(x) = 0 \tag{23}$$



$$F_1(x) = \frac{J_m'(x)}{x} + \frac{K_m'(y)J_m(x)}{\epsilon_r y K_m(y)} \tag{24a}$$

$$F_2(x) = \frac{J_m'(x)}{x} + \frac{K_m'(y)J_m(x)}{y K_m(y)} \tag{24b}$$

$$F_3(x) = \frac{\beta am}{k_0 a \sqrt{\epsilon_r}} J_m(x) \left[\frac{1}{x^2} + \frac{1}{y^2} \right] \tag{24c}$$

$$(23) \quad (18) \quad x \quad \cdot \quad (23) \quad \text{zero가} \quad x$$

(16) x

(25)

x_{\max}

$$x_{\max} = k_0 a \sqrt{\epsilon_r - 1} \quad (25)$$

가 Bessel K_m
 Hankel $H_m^{(2)}$ x_{mn}
 E_{mn} H_{mn} $m=0$ F_3
 (23) (Kajfez 1986).

$$\frac{J_1(x)}{x} + \frac{K_1(y)J_0(x)}{\epsilon_r y K_0(y)} = 0 \quad (26a)$$

$$\frac{J_1(x)}{x} + \frac{K_1(y)J_0(x)}{y K_0(y)} = 0 \quad (26b)$$

(26a) (26b) TM TE $m \neq 0$
 (23) (HEM)

(23) TM TE zero가
 (26)

가 $k_0 a$
 Fig. 2 $k_0 a$

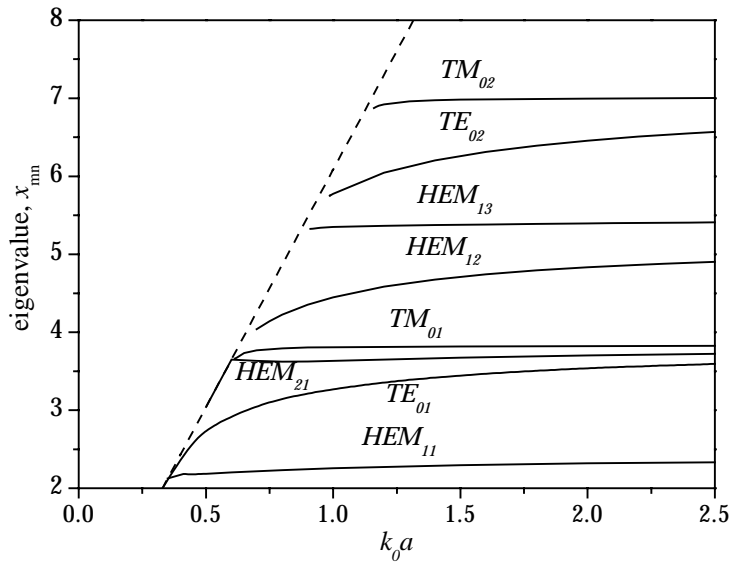


Fig. 2. The eigenvalues of cylindrical dielectric waveguide($\epsilon_r = 10$)



. Fig. 2

$k_0 a$

가

가

가

TM_{01} , HEM_{21} , HEM_{11} TM_{02}

가

가

$k_0 a$

가

가

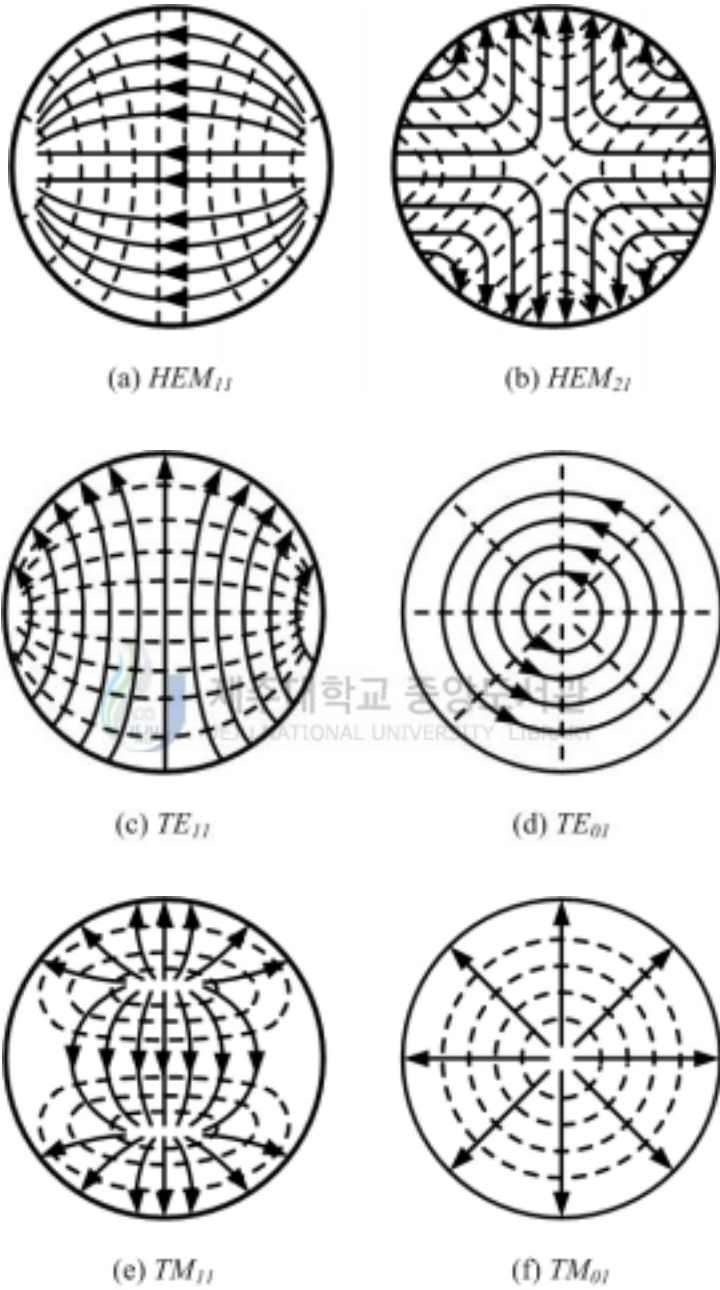


Fig. 3. Cylindrical dielectric waveguide mode patterns

가

Fig. 3

3.

Fig. 4 5

CDRA

CDRA

가

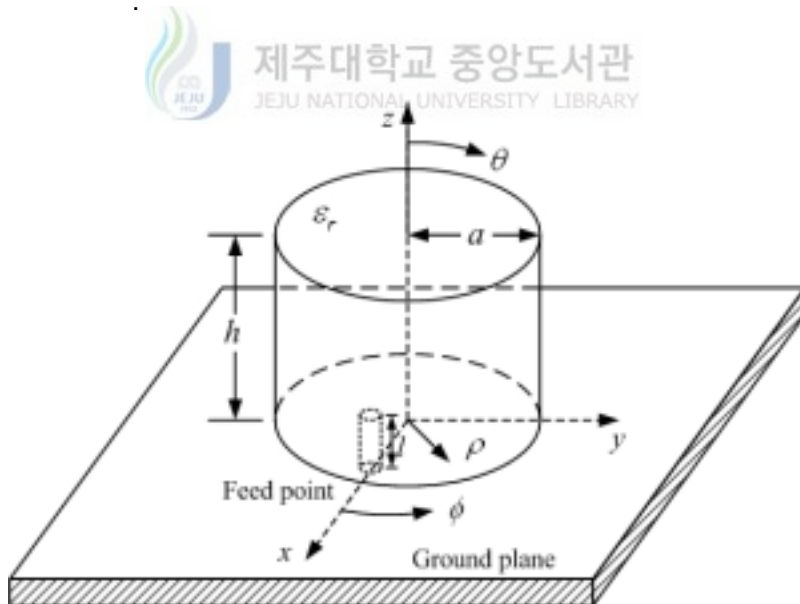


Fig. 4. Geometry of a CDRA

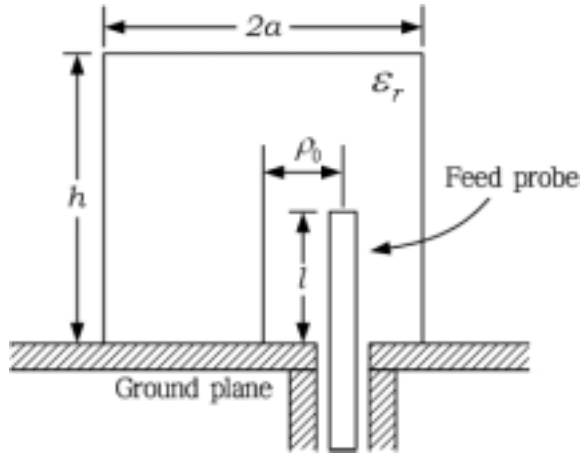


Fig. 5. Feed configuration of a CDRA

가

$$z = -h$$



제주대학교 중앙도서관
JEJU NATIONAL UNIVERSITY LIBRARY

$$z = 0 \quad E_\rho \quad E_\phi$$

1)

가

(cavity)

z

TE

TM

$$\psi_{TE_{mp}} = J_m \left(\frac{x_{mn}}{a} \rho \right) \begin{bmatrix} \sin m\phi \\ \cos m\phi \end{bmatrix} \sin \left[\frac{(2p+1)\pi z}{2h} \right] \quad (27a)$$

$$\psi_{TM_{mp}} = J_m \left(\frac{x'_{mn}}{a} \rho \right) \begin{bmatrix} \sin m\phi \\ \cos m\phi \end{bmatrix} \sin \left[\frac{(2p+1)\pi z}{2h} \right] \quad (27b)$$

J_m 1 m Bessel .

$$J_m(x_{mn}) = 0 \quad (28a)$$

$$J_m'(x'_{mn}) = 0 \quad (28b)$$

$m = 0, 1, 2, 3, \dots$, $n = 1, 2, 3, \dots$, $p = 0, 1, 2, \dots$.

$$k_\rho^2 + k_z^2 = k^2 = \omega^2 \mu \epsilon \quad mnp$$

(Long 1983).

$$f_{mnp} = \frac{1}{2\pi a} \sqrt{\left\{ \begin{matrix} x_{mn}^2 \\ x'_{mn}{}^2 \end{matrix} \right\} + \left[\frac{\pi a}{2h} (2p+1) \right]^2} \quad (29)$$

x_{mn} x'_{mn} TM_{mnp} TE_{mnp} .

2) 가

Maxwell ' s TM_{mnp} TE_{mnp}

TM_{mnp}

$$\begin{aligned}
E_\phi &= \frac{1}{j\omega\epsilon\rho} \frac{\partial^2\psi}{\partial\phi\partial z} \\
&= \frac{n(2p+1)z}{2j\omega\epsilon\rho h} J_m\left(\frac{x'_{mn}}{a}\rho\right) \sin m\phi \sin \frac{(2p+1)\pi z}{2h}
\end{aligned} \tag{30a}$$

$$\begin{aligned}
E_z &= \frac{1}{j\omega\epsilon} \left(\frac{\partial^2}{\partial z^2} + k^2 \right) \psi \\
&= \frac{1}{j\omega\epsilon} \left(\frac{x'_{mn}}{a} \right)^2 J_m\left(\frac{x'_{mn}}{a}\rho\right) \sin m\phi \cos \frac{(2p+1)\pi z}{2h}
\end{aligned} \tag{30b}$$

$$\begin{aligned}
E_\rho &= \frac{1}{j\omega\epsilon} \frac{\partial^2\psi}{\partial\rho\partial z} \\
&= \frac{-\pi x'_{mn}(2p+1)}{2j\omega\epsilon ah} J'_m\left(\frac{x'_{mn}}{a}\rho\right) \cos m\phi \sin \frac{(2p+1)\pi z}{2h}
\end{aligned} \tag{30c}$$

TE_{mnp}



$$\begin{aligned}
H_\phi &= \frac{1}{j\omega\mu\rho} \frac{\partial^2\psi}{\partial\phi\partial z} \\
&= -\frac{1}{j\omega\mu\rho} \frac{m(2p+1)\pi}{2h} J_m\left(\frac{x_{mn}}{a}\rho\right) \sin m\phi \cos \frac{(2p+1)\pi z}{2h}
\end{aligned} \tag{31a}$$

$$\begin{aligned}
H_z &= \frac{1}{j\omega\mu} \left(\frac{\partial^2}{\partial z^2} + k^2 \right) \psi \\
&= \frac{1}{j\omega\mu} \left(\frac{x_{mn}}{a} \right)^2 J_m\left(\frac{x_{mn}}{a}\rho\right) \cos m\phi \sin \frac{(2p+1)\pi z}{2h}
\end{aligned} \tag{31b}$$

$$\begin{aligned}
H_\rho &= \frac{1}{j\omega\mu} \frac{\partial^2\psi}{\partial\rho\partial z} \\
&= \frac{1}{j\omega\mu} \left(\frac{x_{np}}{a} \right) \frac{(2p+1)\pi z}{2d} J'_m\left(\frac{x_{mn}}{a}\rho\right) \cos m\phi \cos \frac{(2p+1)\pi z}{2h}
\end{aligned} \tag{31c}$$

$$\rho, \phi, z \quad k = \sqrt{\mu\epsilon} \quad (30) \quad (31)$$

$$\vec{M} = \vec{E} \times \vec{n} \quad \text{S} \quad \vec{n}$$

$$\vec{M} = \vec{\rho} \times [\vec{\phi} E_\phi + \vec{z} E_z] : \text{side} \quad (32a)$$

$$\vec{M} = \vec{z} \times [\vec{\rho} E_\rho + \vec{\phi} E_\phi] : \text{Top, Bottom} \quad (32b)$$

source 가

side :

$$M_z = \frac{n(2p+1)\pi}{2j\omega\epsilon ah} J_m(x'_{mn}) \sin m\phi' \sin \frac{(2p+1)\pi z'}{2h} \quad (33a)$$

$$M_{\phi'} = \frac{1}{j\omega\epsilon} \left(\frac{x'_{mn}}{a} \right)^2 J_m(x'_{mn}) \cos m\phi' \cos \frac{(2p+1)\pi z'}{2h} \quad (33b)$$

Top bottom :

$$M_{\phi'} = \frac{(2p+1)\pi x'_{mn}}{j2\omega\epsilon ah} J_m\left(\frac{x'_{mn}}{a} \rho'\right) \cos m\phi' \quad (34a)$$

$$M_{\rho'} = \frac{(2p+1)m\pi}{j2\omega\epsilon h \rho'} \left(\frac{x'_{mn}}{a} \right)^2 J_m\left(\frac{x'_{mn}}{a} \rho'\right) \sin m\phi' \quad (34b)$$

3) Far - field

far - field source

$$M_{\theta} = M'_{\rho} \cos \theta \cos(\phi - \phi') + M'_{\phi} \cos \theta \sin(\phi - \phi') - M'_z \sin \theta \quad (35a)$$

$$M_{\phi} = -M'_{\rho} \sin(\phi - \phi') + M'_{\phi} \cos(\phi - \phi') \quad (35b)$$

$$F_{\theta} = \frac{e^{-jk_0 r}}{4\pi r} \iiint M_{\theta} e^{jk_0[\rho' \sin \theta \cos(\phi - \phi') + z' \cos \theta]} \rho' d\rho' d\phi' dz' \quad (36a)$$

$$F_{\phi} = \frac{e^{-jk_0 r}}{4\pi r} \iiint M_{\phi} e^{jk_0[\rho' \sin \theta \cos(\phi - \phi') + z' \cos \theta]} \rho' d\rho' d\phi' dz' \quad (36b)$$

$$k_0 = \omega \sqrt{\mu_0 \epsilon_0} \quad M_{\theta} \quad M_{\phi}$$

$$F_{\theta} = C_1 \left\{ I_2 - I_1 - 0.5k_{\rho} (I_3 + I_4 - I_5 - I_6) \right. \\ \left. + 1.16k_0 \sin \theta J_1(k_0 a \sin \theta) D_1 \right. \\ \left. - 0.581k_{\rho}^2 a [J_0(k_0 a \sin \theta) + J_2(k_0 \sin \theta)] D_1 \right\} \quad (37a)$$

$$F_{\phi} = C_2 \left\{ -I_1 - I_2 - 0.5k_{\rho} (I_3 - I_4 - I_5 + I_6) \right. \\ \left. - 0.581k_{\rho}^2 a [J_0(k_0 a \sin \theta) - J_2(k_0 \sin \theta)] D_1 \right\} \quad (37b)$$

$$C_1 = \frac{\pi^2}{j\omega\epsilon d} \frac{1}{4\pi r} \sin\phi \cos(k_0 d \cos\theta) \cos\theta \quad (38a)$$

$$C_2 = \frac{\pi^2}{j\omega\epsilon d} \frac{1}{4\pi r} \cos\phi \cos(k_0 d \cos\theta) \quad (38b)$$

$$D_1 = \left[\frac{\pi^2}{4d^2} - k_0^2 \cos^2\theta \right]^{-1} \quad (39)$$

$$k_\rho = \frac{x'_{11}}{a} = \frac{3.8317}{a} \quad (40)$$

$$I_1 = \int_0^a J_1(k_\rho \rho') J_0(k_0 \rho' \sin\theta) d\rho' \quad (41a)$$

$$I_2 = \int_0^a J_1(k_\rho \rho') J_2(k_0 \rho' \sin\theta) d\rho' \quad (41b)$$

$$I_3 = \int_0^a J_0(k_\rho \rho') J_0(k_0 \rho' \sin\theta) d\rho' \quad (41c)$$

$$I_4 = \int_0^a J_0(k_\rho \rho') J_2(k_0 \rho' \sin\theta) d\rho' \quad (41d)$$

$$I_5 = \int_0^a J_2(k_\rho \rho') J_0(k_0 \rho' \sin\theta) d\rho' \quad (41e)$$

$$I_6 = \int_0^a J_2(k_\rho \rho') J_2(k_0 \rho' \sin\theta) d\rho' \quad (41f)$$

Far - field

$$\vec{F} : E_\theta \propto F_\phi \quad E_\phi \propto F_\theta$$

Fig. 6

$\epsilon_r = 10$, $a = 10.65$ mm, $h = 10.6$ mm CDRA

$TM_{01\delta}$

$TM_{01\delta}$ 3.8317

5.875GHz

near - field Fig. 7

$TM_{01\delta}$ $HEM_{11\delta}$

Fig.

8 Fig. 9

$TM_{01\delta}$

$\lambda/4$

$HEM_{11\delta}$

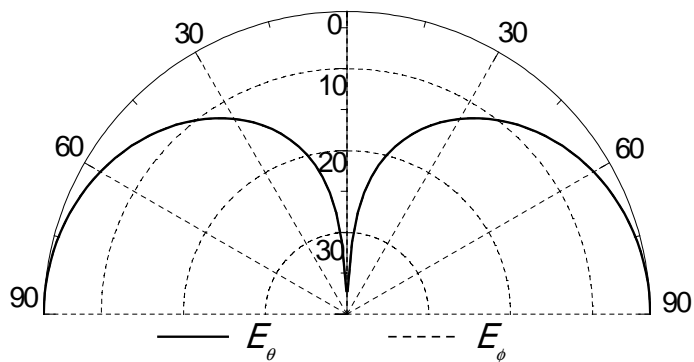


Fig. 6. Calculated radiation patterns of CDRA

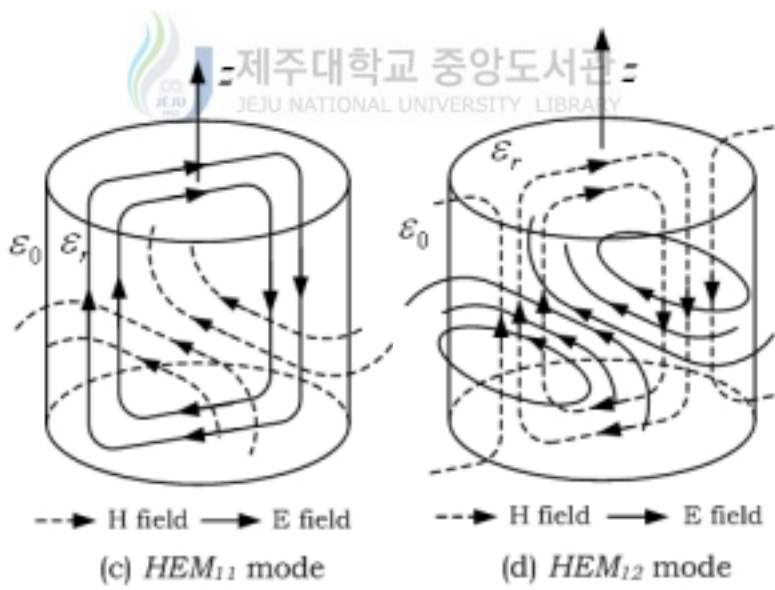
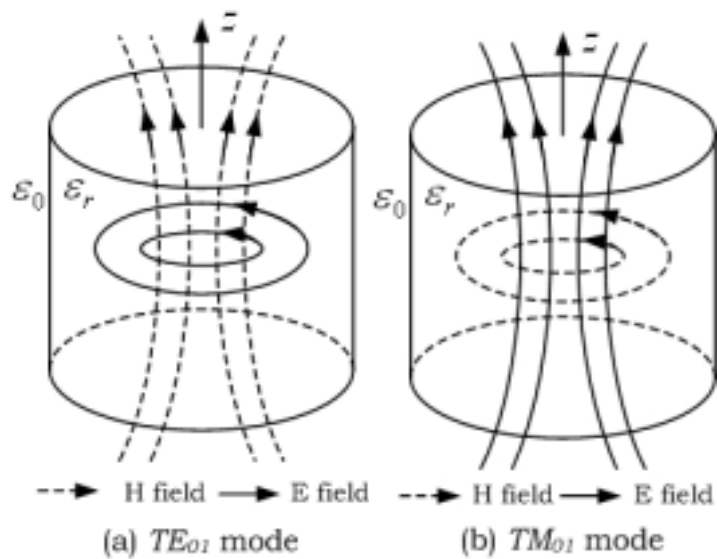


Fig. 7. Sketch for the field distributions of cylindrical dielectric waveguide

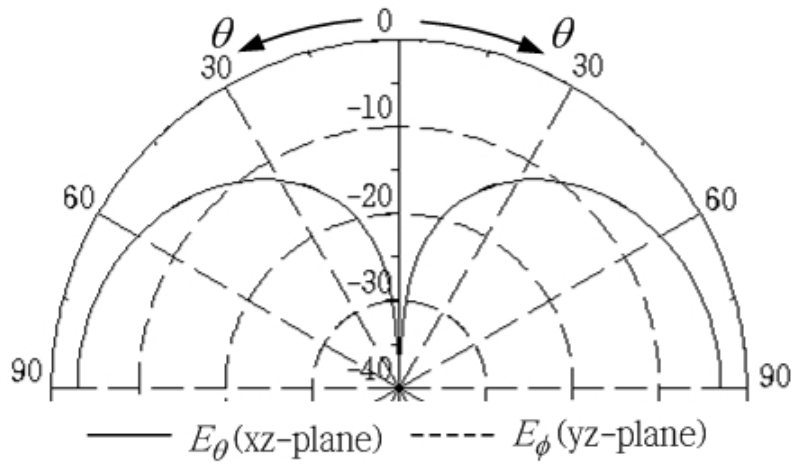


Fig. 8. Ideal radiation patterns for the $TM_{01\delta}$ mode above infinite ground plane

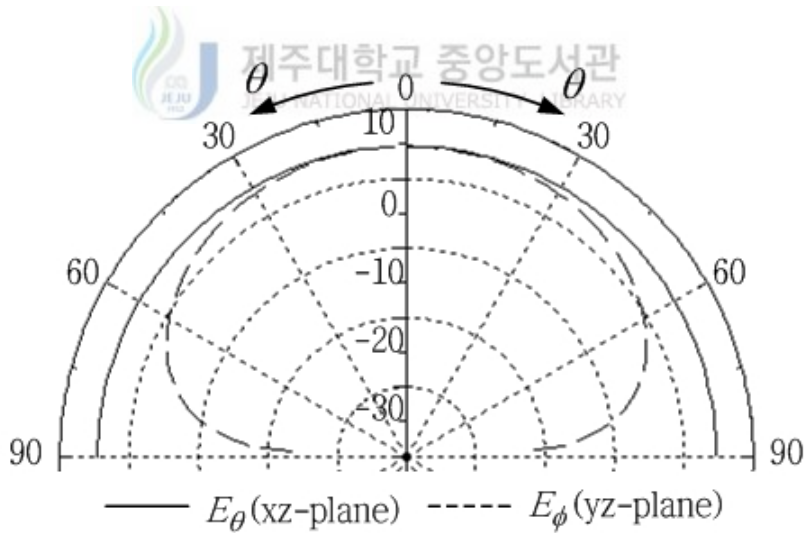


Fig. 9. Ideal radiation patterns for the $HEM_{11\delta}$ mode above infinite ground plane

4. CDRA

CDRA

, Kishk (1985), Martin (1990)

CPW(Co-planar waveguide)

CDRA

가

가

CDRA

가

1)

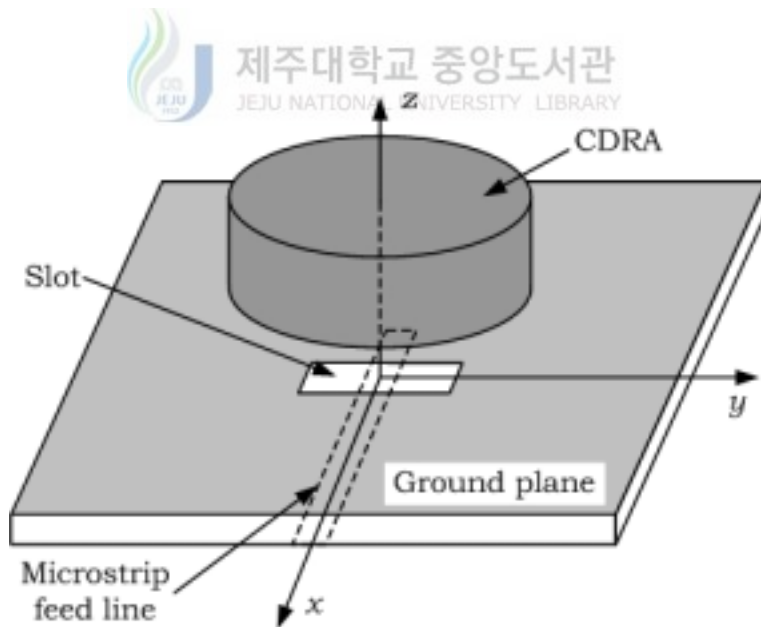


Fig. 10. Geometry of aperture - coupled CDRA

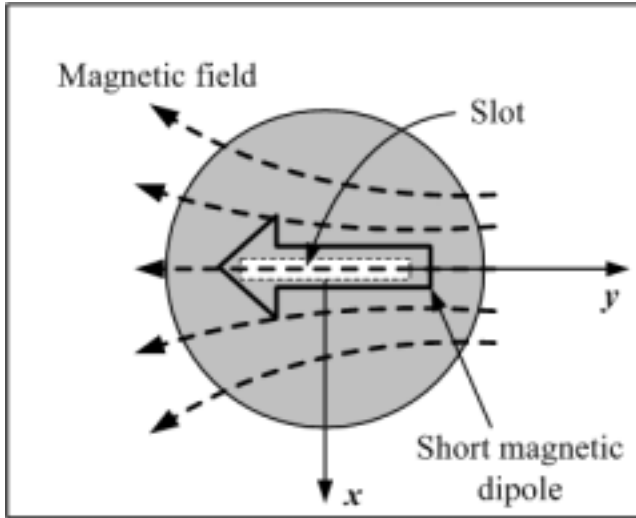


Fig. 11. Equivalent model of aperture - coupled CDRA

CDRA 가 Fig. 10 Fig. 11



DRA

가

Fig.

11

CDRA

Fig. 12

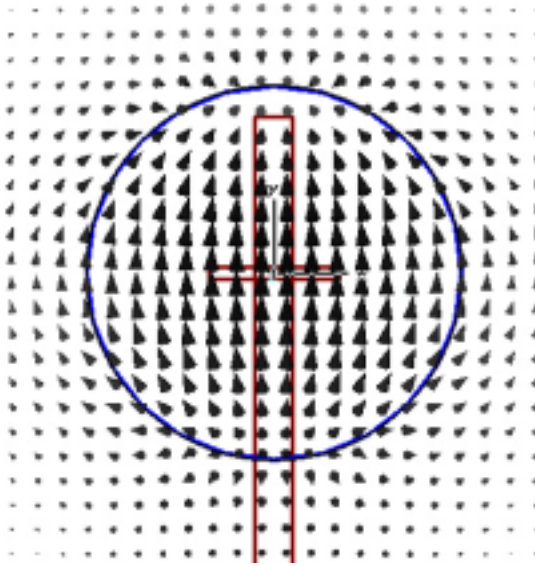
$HEM_{11\delta}$

가

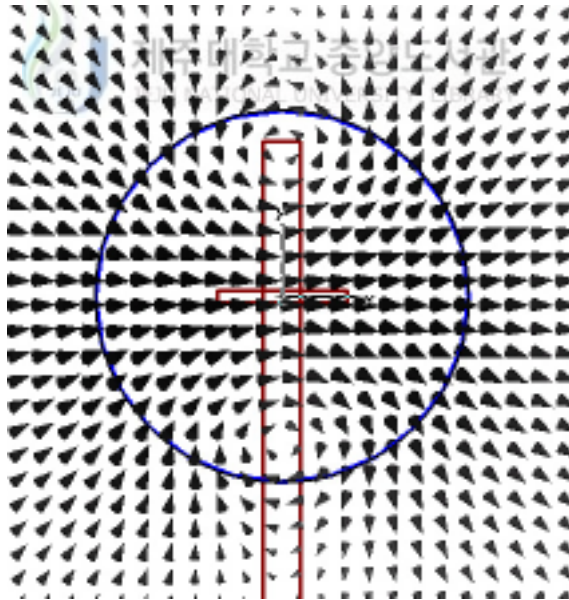
가

CDRA

(, 2001).



(a) E - field



(b) H - field

Fig. 12. The field distribution of aperture - fed CDRA

CDRA
 (Leung 1999), (Martin 1990). CDRA
 L 가
 L -

2)

CDRA

Fig. 13

CDRA

가

CDRA

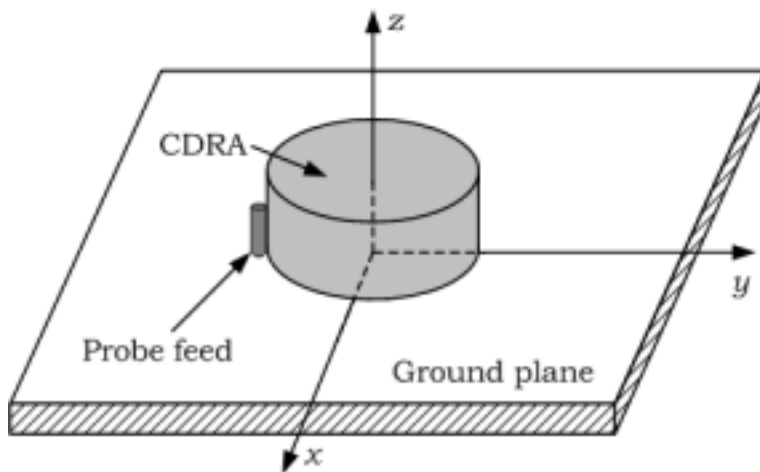


Fig. 13. Geometry of Coaxial probe - fed CDRA

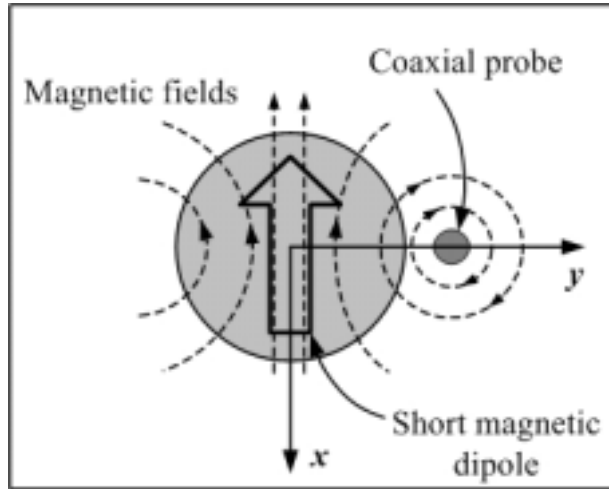
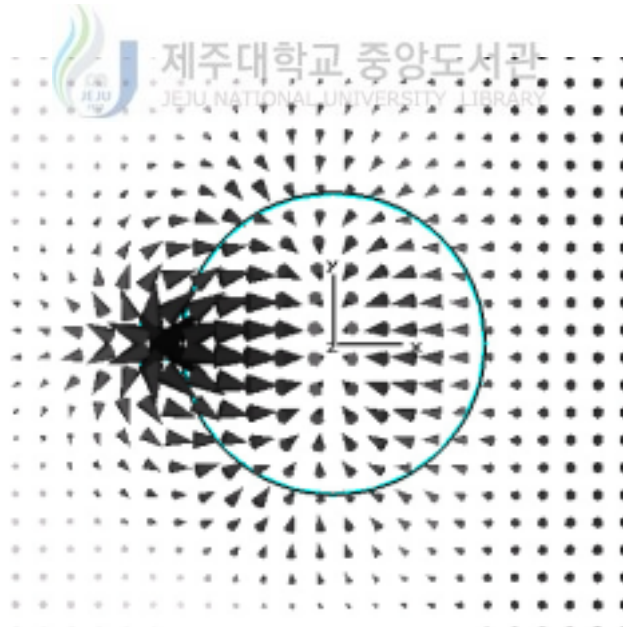
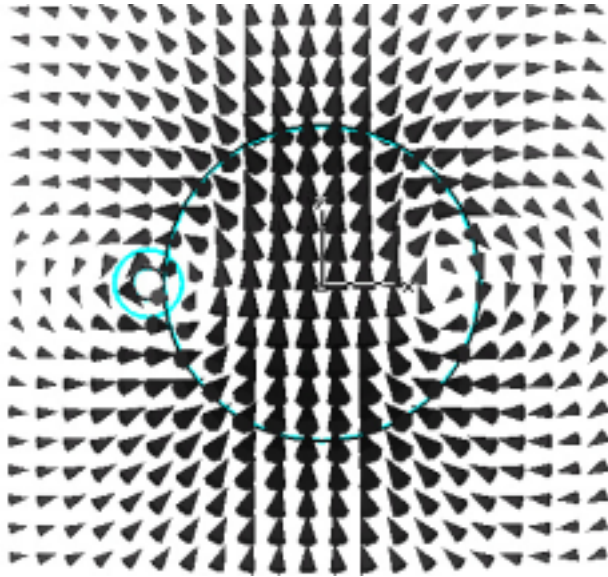


Fig. 14. Equivalent model of coaxial probe - fed CDRA



(a) E - field



(b) H - field

Fig. 15. The field distribution of a probe - fed CDRA



DRA

(RDRA; rectangular dielectric resonator antenna)

$TE_{01\delta}$

가

CDRA

Fig. 14

$HEM_{11\delta}$ (

)가

Fig. 15

. CDRA

$TM_{01\delta}$

가

50

가

가

3)

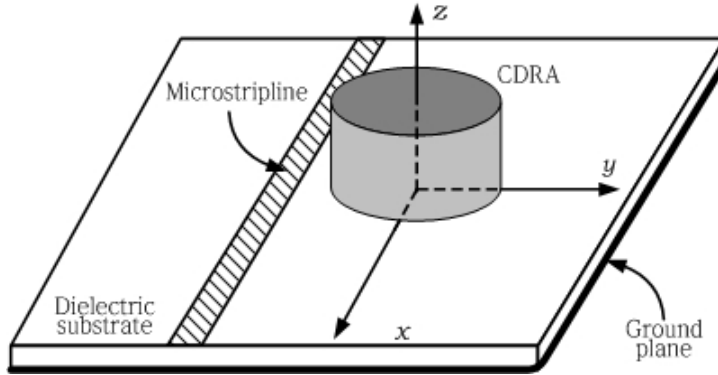


Fig. 16. Geometry of Microstrip line fed CDRA

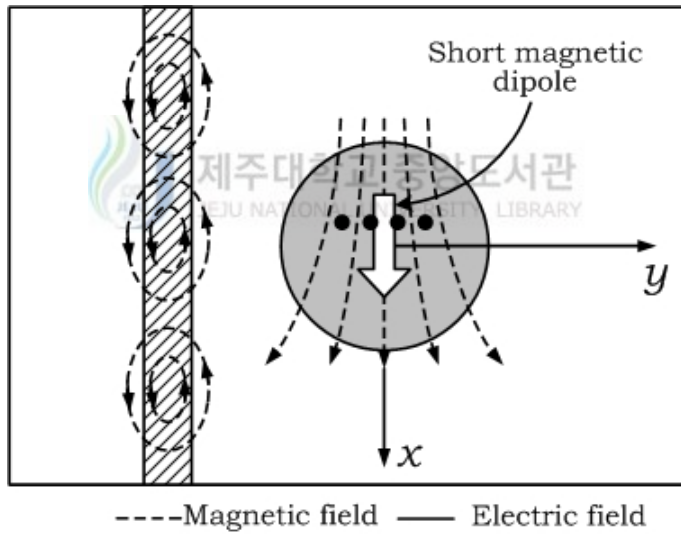


Fig. 17. Equivalent model of microstrip line fed CDRA

CDRA

(Leung 1997).

Fig. 16

Fig. 17

가

CDRA

DRA

CDRA

4) (loop)

CDRA

Fig. 18

CDRA

CDRA

Fig. 19

CDRA

CDRA

CDRA $HEM_{11\delta}$

$TE_{01\delta}$

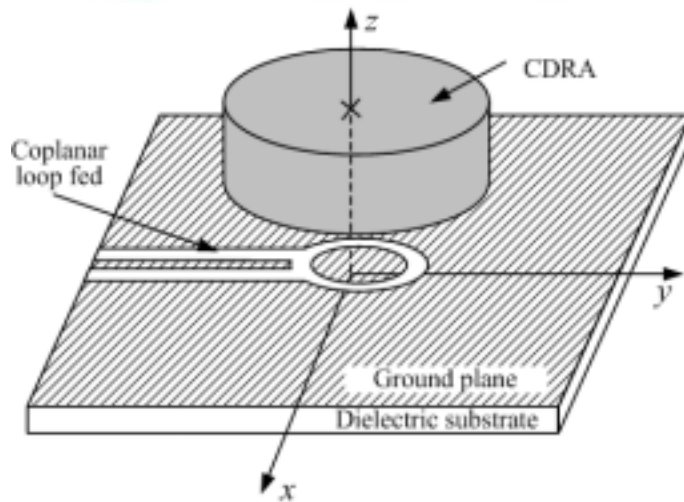


Fig. 18. Geometry of co - planar loop - fed CDRA

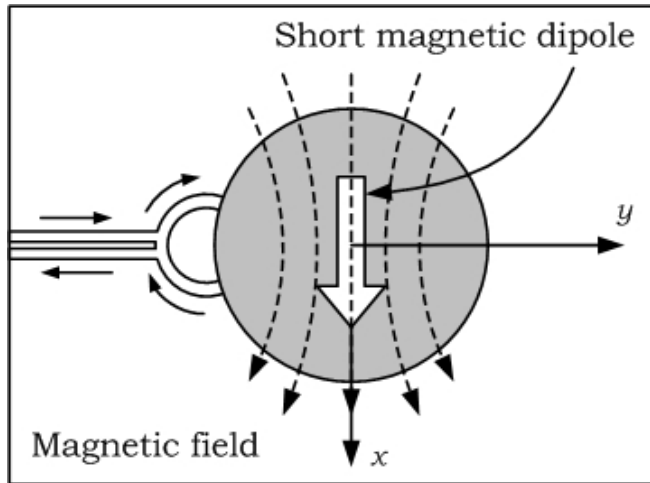


Fig. 19. Equivalent model of co-planar loop - fed CDRA

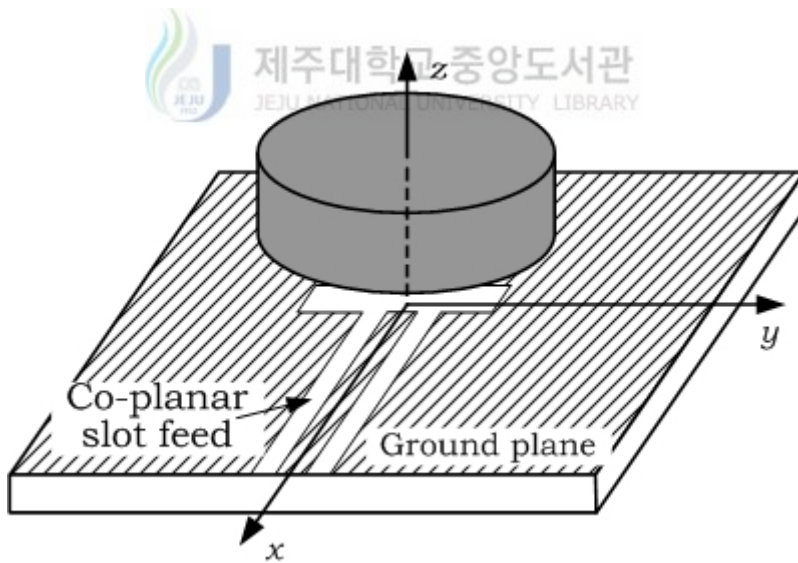


Fig. 20. Geometry of Co-planar slot - fed CDRA

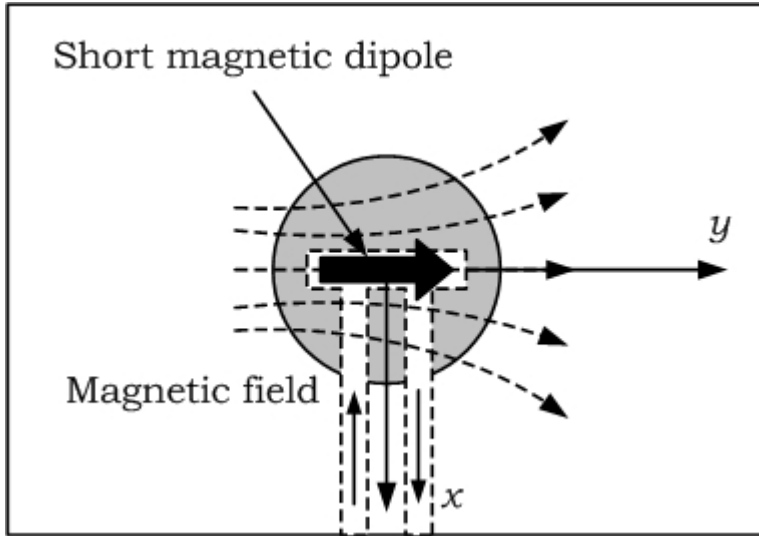


Fig. 21. Equivalent of Co - planar slot - fed CDRA

Fig. 20 Fig. 21 (slot) DRA
 . Fig. 21 가 JEJU NATIONAL UNIVERSITY LIBRARY
 CDRA

III.

1.

CDRA

Fig. 22 CDRA

CDRA

Q

(Kishk Glisson, 2001).

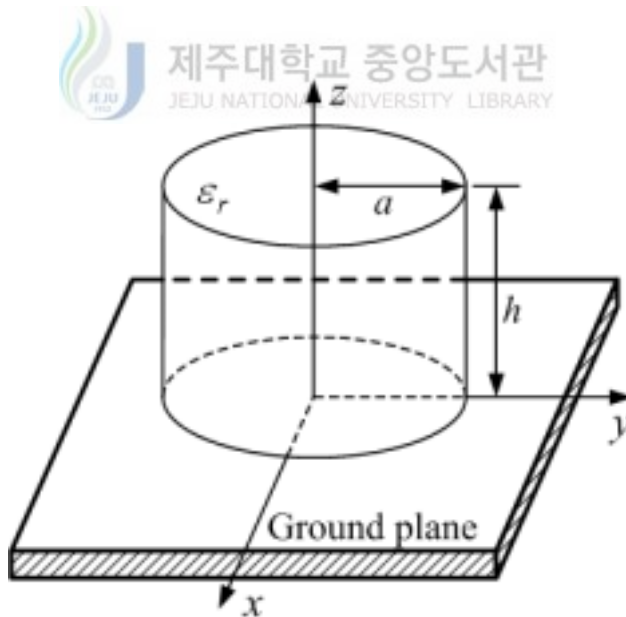


Fig. 22. The CDRA mounted on a ground plane

$TE_{01\delta}$ Mode :

$$f_0 = \frac{2.921c\epsilon_r^{-0.465}}{2\pi a} \left[0.691 + 0.319 \left(\frac{a}{2h} \right) - 0.035 \left(\frac{a}{2h} \right)^2 \right] \quad (42a)$$

$$Q = 0.012\epsilon_r^{1.2076} \left[5.270 \left(\frac{a}{2h} \right) + 1106.188 \left(\frac{a}{2h} \right)^{0.625} e^{-1.0272 \left(\frac{a}{2h} \right)} \right] \quad (42b)$$

$HEM_{11\delta}$ Mode :

$$f_0 = \frac{2.735c\epsilon_r^{-0.463}}{2\pi a} \left[0.543 + 0.589 \left(\frac{a}{2h} \right) - 0.05 \left(\frac{a}{2h} \right)^2 \right] \quad (43a)$$

$$Q = 0.013\epsilon_r^{1.202} \left[2.135 \left(\frac{a}{2h} \right) + 228.043 \left(\frac{a}{2h} \right)^{-2.046} e^{0.111 \left(\frac{a}{2h} \right)^2} \right] \quad (43b)$$

$TM_{01\delta}$ Mode :

$$f_0 = \frac{2.933c\epsilon_r^{-0.468}}{2\pi a} \left\{ 1 - \left[0.075 + 0.05 \left(\frac{a}{2h} \right) \right] \left(\frac{\epsilon_r - 10}{28} \right) \right\} \cdot \left\{ 1.048 + 0.377 \left(\frac{a}{2h} \right) - 0.071 \left(\frac{a}{2h} \right)^2 \right\} \quad (44a)$$

$$Q = 0.009\epsilon_r^{0.888} e^{0.04\epsilon_r} \left\{ 1 - \left[0.3 - 0.2 \left(\frac{a}{2h} \right) \right] \left[\frac{38 - \epsilon_r}{28} \right] \right\} \cdot \left\{ 9.498 \left(\frac{a}{2h} \right) + 2058.33 \left(\frac{a}{2h} \right)^{4.322} e^{-3.501 \left(\frac{a}{2h} \right)} \right\} \quad (44b)$$

a h DRA DRA
 (BW) Q

$$BW = \frac{S-1}{Q\sqrt{S}} \cdot 100 \text{ [%]} \quad (45)$$

Fig. 23 $\epsilon_r = 10$ VSWR a/h
 $TE_{01\delta}$ $TM_{01\delta}$ 가 가
 $HEM_{01\delta}$ 가

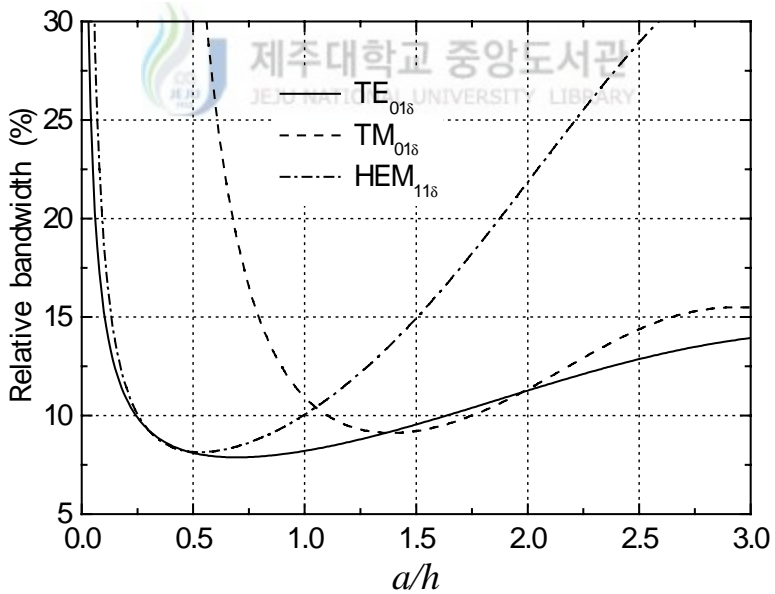


Fig. 23. Relative bandwidth of CDRAs with $\epsilon_r = 10$

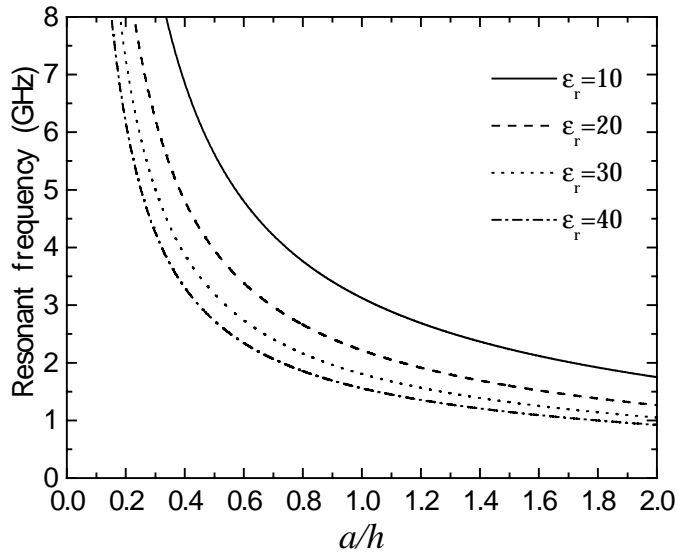


Fig. 24. Resonant frequency for the $TM_{01\delta}$ mode of CDRA



Q

Q

· $\epsilon_r = 1$ DRA Q 가
DRA · DRA

가

· Fig. 24, Fig. 25 Fig. 26 $TM_{01\delta}$ CDRA , Q

· Fig. 24

$\epsilon_r = 10, 20, 30, 40$

a/h

a/h 가 가

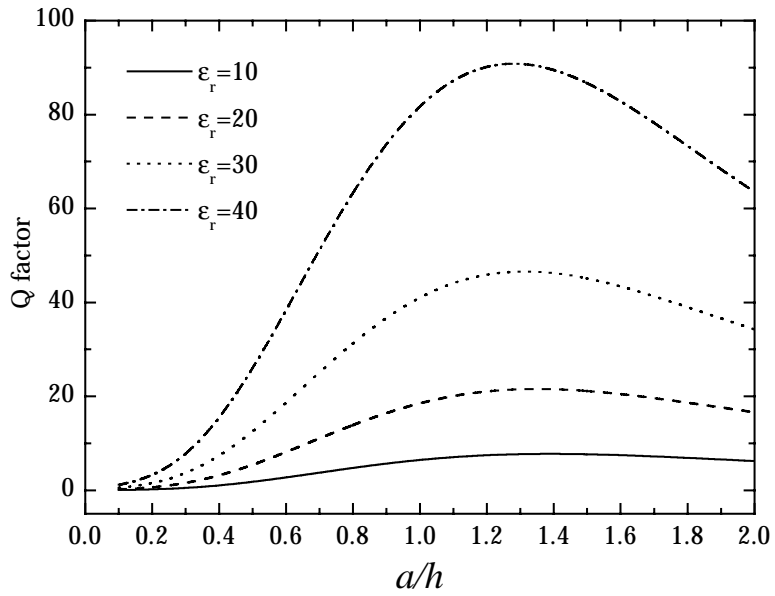


Fig. 25. Radiation Q - factor for the $TM_{01\delta}$ mode of CDRA



가 CDRA a/h

, CDRA DR

가

가

Fig. 25

Fig. 26

a/h

Q

Q

a/h 가 가

Fig. 25

a/h=1.25

가 가

Q

a/h Q

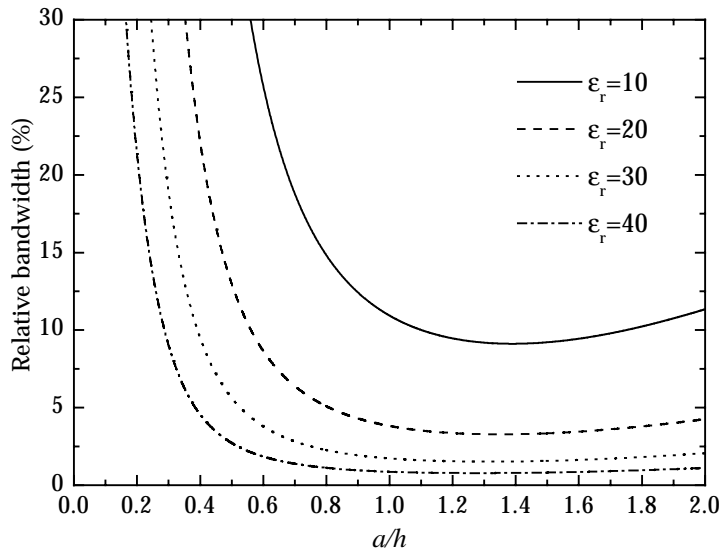


Fig. 26. Relative bandwidth for the $TM_{01\delta}$ mode of CDRA



가 Q 가 가 ,
 $\epsilon_r = 10$ 4 가 1/10

. Fig. 25 ($\epsilon_r \approx 10$)

($\epsilon_r > 20$)

DRA a/h Q 가
 가 .

Fig. 26 a/h

Table 1 . 20

Table 1. Minimum bandwidth for each relative permittivity

ϵ_r	10	20	30	40
Minimum Bandwidth(%)	9.1	3.3	1.52	0.8

2.



1) DRA

Fig. 27

DRA

TM_{01δ}

Fig. 28

Fig. 27

가

가

Fig. 28

Fig. 27

Fig. 28

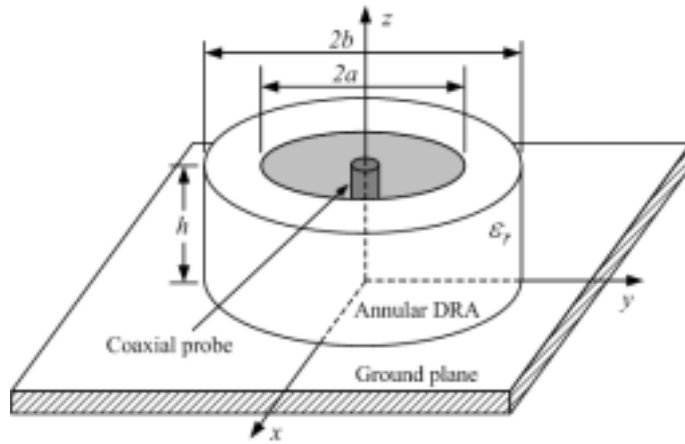


Fig. 27. Geometry of the annular DRA

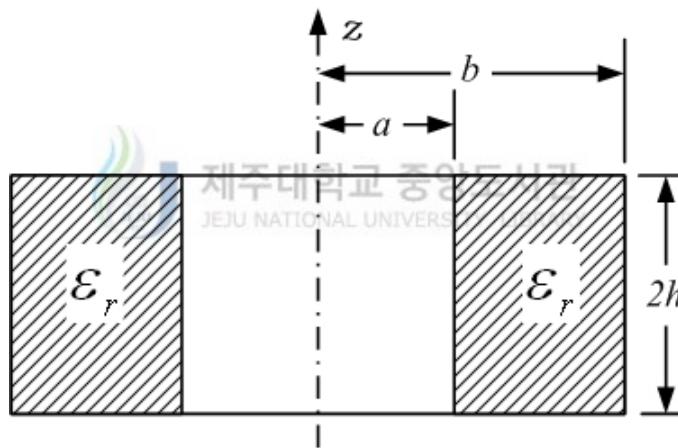


Fig. 28. Equivalent model of the annular DRA

Fig. 28

ψ

$$\psi_{TM_{mn}} = B_{mn} \sin \frac{n\pi z}{2h} R_m \left(x_{mn} \frac{r}{b} \right) \quad (46)$$

$$R_m \quad \text{Bessel} \quad R_m$$

$$R_m = J_m(z) + CY_m(z) \quad (47)$$

$$x \qquad \qquad \qquad r = b \qquad \psi = 0$$

$$R_m(x_{mn}) = 0 \tag{48}$$

$$r = a \qquad \psi = 0$$

$$R_m\left(\frac{a}{b}x_{mn}\right) = 0 \tag{49}$$

$$(48) \qquad (49)$$

$$\frac{J_1(x_{11})}{Y_1(x_{11})} = \frac{J_1\left(\frac{a}{b}x_{11}\right)}{Y_1\left(\frac{a}{b}x_{11}\right)} \tag{50}$$



$$k_{mn}^2 = \left(\frac{n\pi}{2h}\right)^2 + \left(\frac{x_{mn}}{b}\right)^2 \tag{51}$$

(51)

$$f = \frac{c}{2\pi\sqrt{\epsilon_r}} \sqrt{\left(\frac{\pi}{2h}\right)^2 + \left(\frac{x_{mn}}{b}\right)^2} \tag{52}$$

$$c = 1/\sqrt{\mu_0\epsilon_0}$$

a/b

x_{11}

Table 2

Fig. 29

Table 2. Values of x_{11} for various ratios for a/b

a/b	x_{11}	a/b	x_{11}
0.0	3.8317	0.5	6.3932
0.1	3.9409	0.6	7.9301
0.2	4.2358	0.7	10.5220
0.3	4.7058	0.8	15.7376
0.4	5.3912	0.9	31.4292

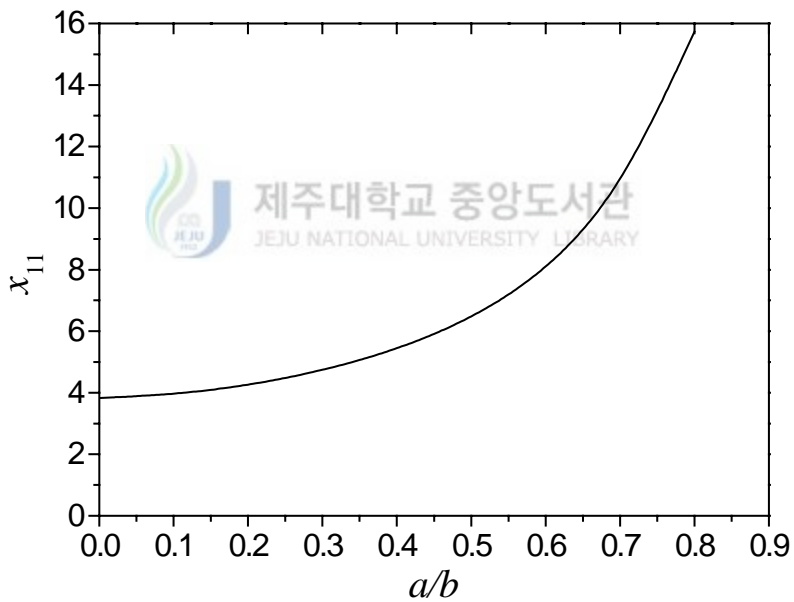


Fig. 29. Solution of x_{11} for values of a/b

$$\varepsilon_r = 36.2, \quad b = 5.975 \text{ mm}, \quad h = 5.4 \text{ mm}$$

DRA

a/b

Table 3

Fig. 30

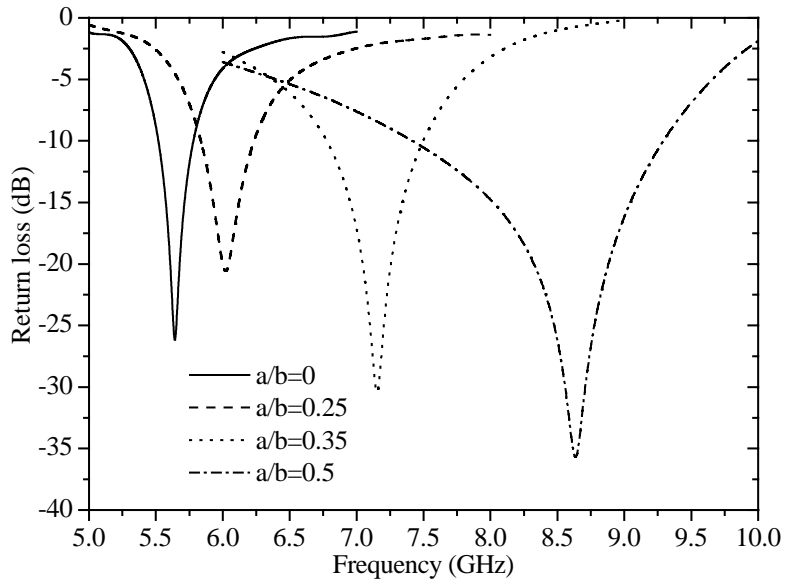


Fig. 30. Return loss of annular DRA according to a/b

Table 3. Effect of a/b on the resonant frequency and bandwidth of annular DRA

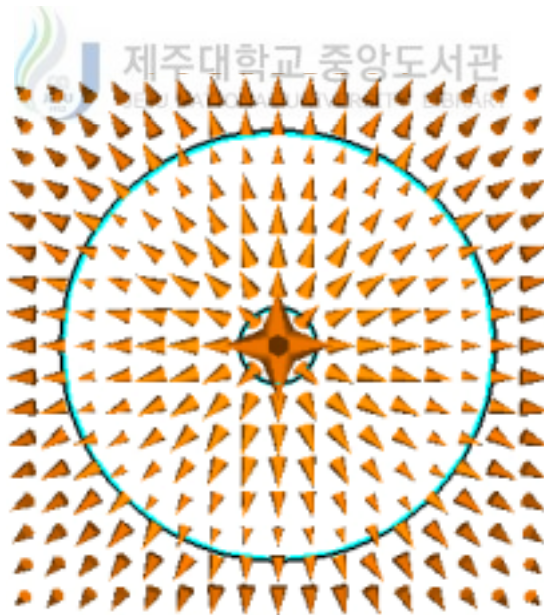
a/b	Resonant frequency f_r (GHz)	Frequency Range (GHz)	Bandwidth (%)
0.0	5.63	5.5~5.77	4.8
0.25	6.02	5.8~6.23	7.1
0.35	7.15	6.77~7.5	10.2
0.5	8.64	7.4~9.3	22

a/b 가 가 가 가 . a/b 가 가 가 (air gap) DRA

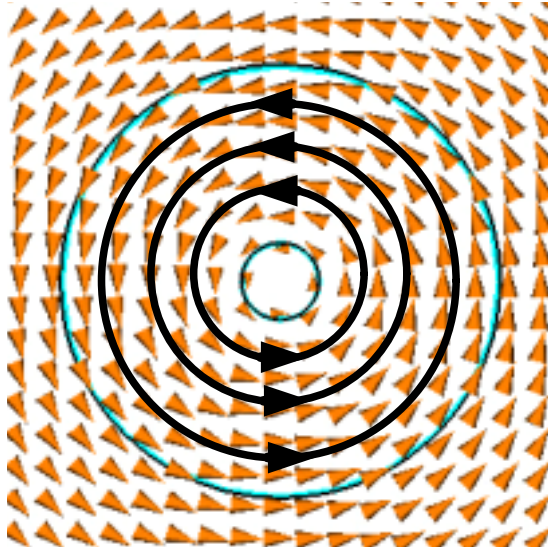
$\epsilon_r = 36$ $a = 6.9 \text{ mm}$, $h = 6.2 \text{ mm}$ $a/b = 0.152$ 5.6GHz
 DRA 2mm 4mm 가 6.5%
 11.5% 가 (Shum Luk, 1994).

2) DRA

Fig. 31 DRA z
 가 CDRA
 $TM_{01\delta}$ DRA $TM_{01\delta}$ 가
 Fig. 32 $TM_{01\delta}$



(a) E - field



(b) H - field

Fig. 31. The field distribution for the annular DRA

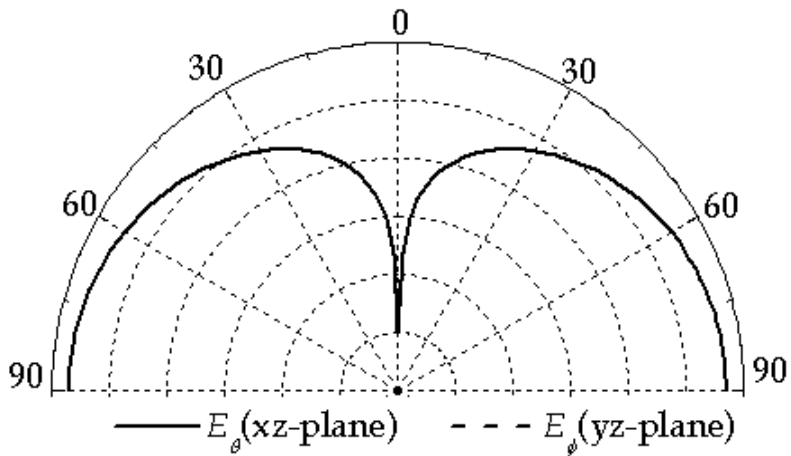


Fig. 32. The radiation patterns for the annular DRA

3.

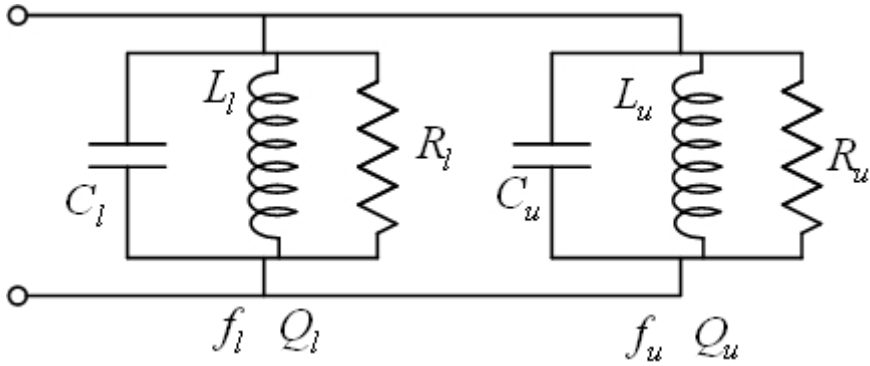


Fig. 33. Lumped element impedance model for a two - DRA configuration



DRA가

(Fan Antar, 1997).

DRA

Fig. 33

RLC

가

f_u, f_l, Q_u, Q_l

가 . Fig. 34(a)

, 가

Fig. 34(b)

. Fig. 34(c)

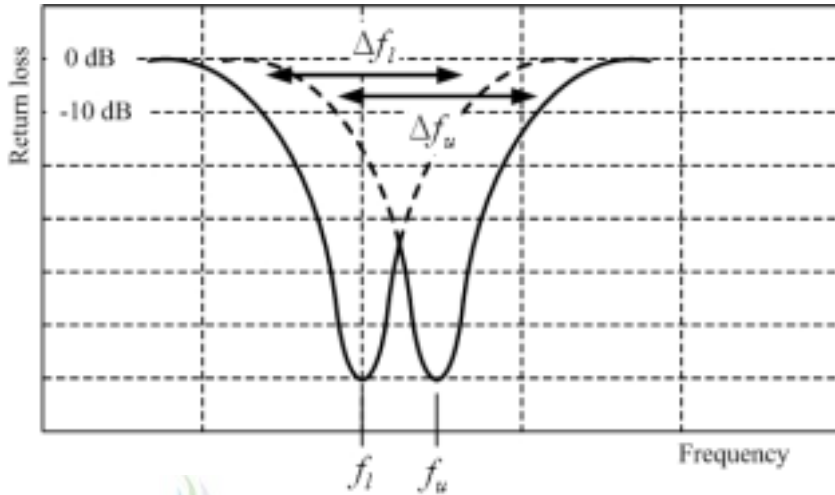
.(Luk Leung, 2003)

$$(\Delta f_u + \Delta f_l) = 2(f_u - f_l) \quad (53)$$

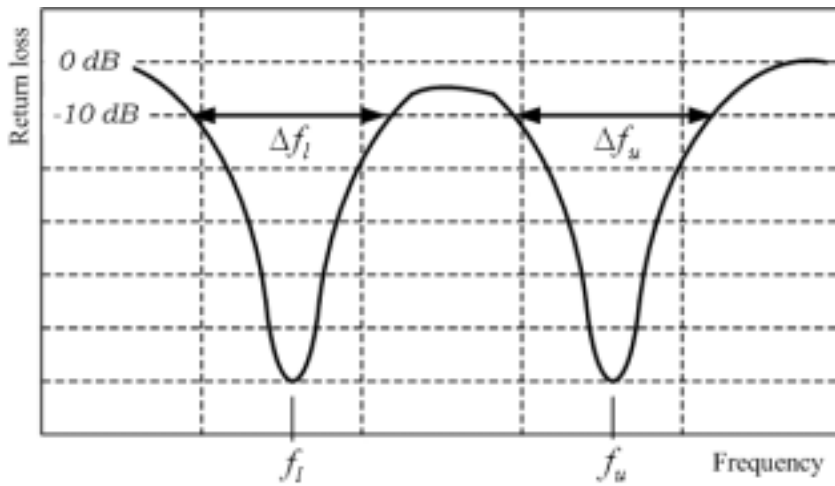
$$\Delta f \quad 10 \text{ dB} \quad (53) \quad Q$$

가 .

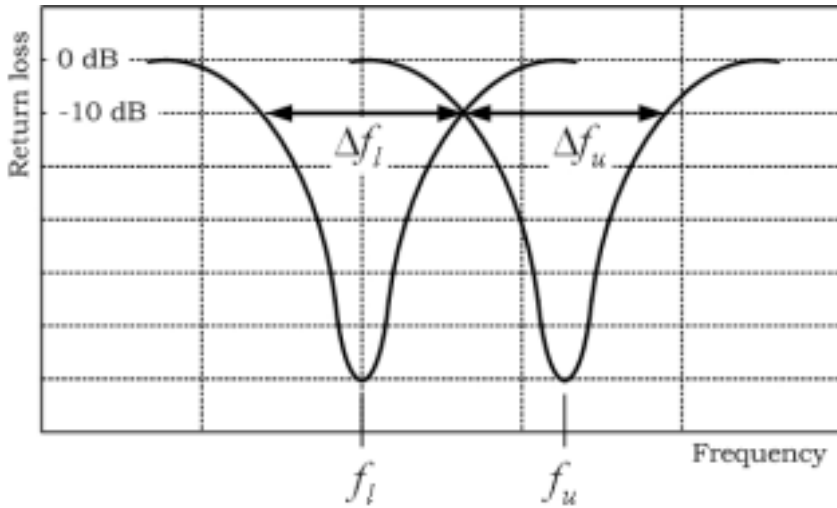
$$\left(\frac{f_u}{Q_u} + \frac{f_l}{Q_l}\right) = 2(f_u - f_l) \quad (54)$$



(a) Broadband response $(\Delta f_u + \Delta f_l) > 2(f_u - f_l)$



(b) Dual - band response $(\Delta f_u + \Delta f_l) < 2(f_u - f_l)$



(c) Two - resonator response $(\Delta f_u + \Delta f_l) = 2(f_u - f_l)$

Fig. 34. Dual band and broadband response for a two - DRA configuration



(53)

Q

가

Fig. 34(c)

(53)

$$(\Delta f_u + \Delta f_l) > 2(f_u - f_l)$$

$$(\Delta f_u + \Delta f_l) < 2(f_u - f_l)$$

DRA

Fig. 35

Fig. 36

DRA

DRA

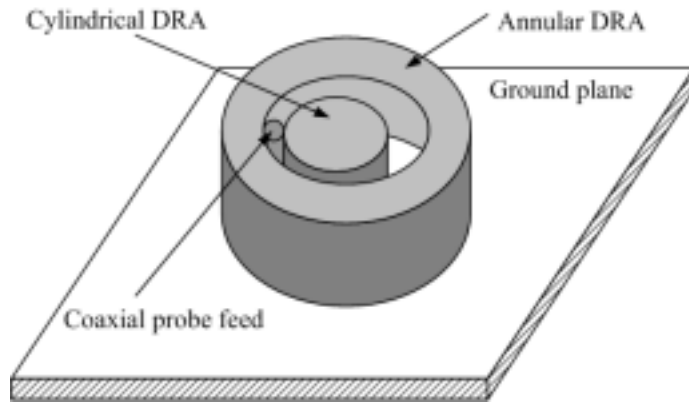


Fig. 35. Annular DRA with embedded CDRA

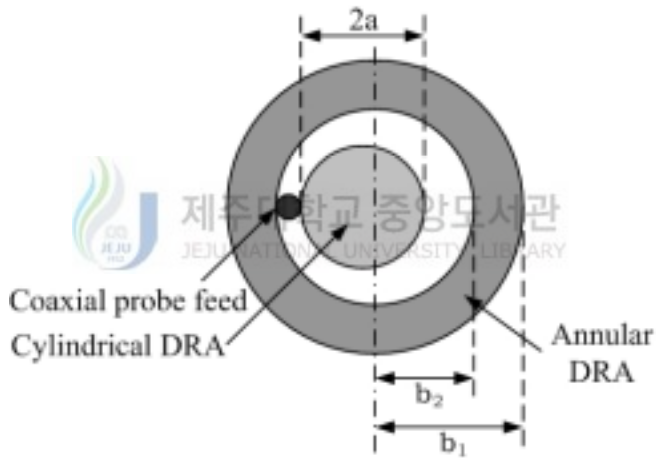


Fig. 36. Top views of annular DRA with embedded CDRA

Q CDRA DRA 가
(53)

$$2a_1 = 12\text{mm} , h = 2\text{mm} , \epsilon_{r1} = 30.5 , a_2 = 12\text{mm} , b_2 = 8\text{mm}$$

$$\epsilon_{r2} = 36.7$$

38%

4mm (Sangiovani 1997).

IV.

1. CDRA

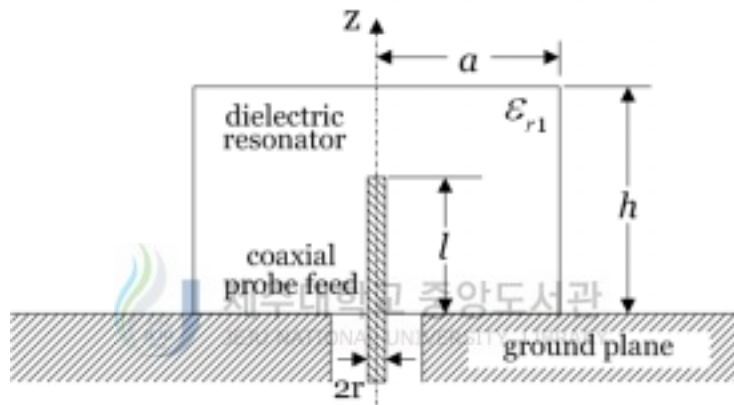


Fig. 37. Geometry of a probe - fed CDRA

Fig. 37 ϵ_{r1} , 가 a , h
 $2r$ 가 l
 CDRA .

Table 4 .

Table 4. Design parameters of a CDRA

Relative permittivity (ϵ_{r1})	Radius (a)	Height (h)	Probe length (l)	Probe radius (r)
10	10.65mm	10.6mm	4.5mm	0.813mm

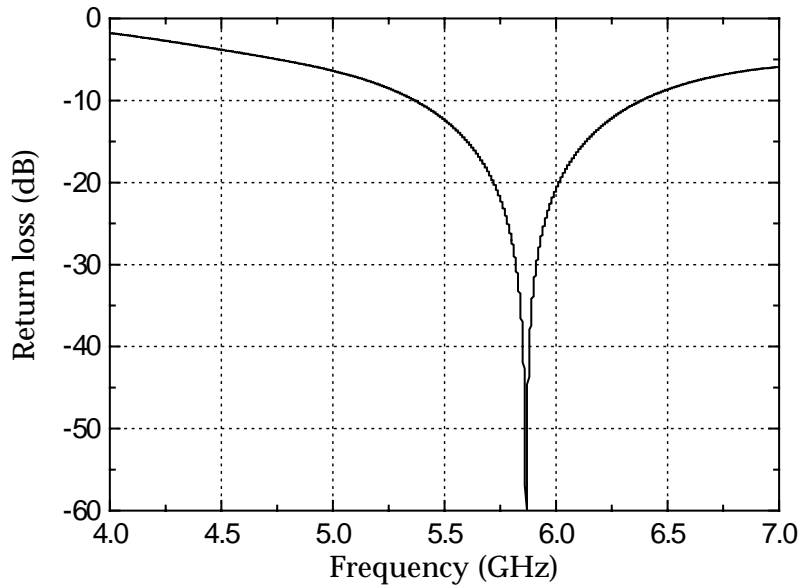


Fig. 38. The return loss of CDRA
 제주대학교 중앙도서관
 JEJU NATIONAL UNIVERSITY LIBRARY

(43a)

Table 4

5.873

GHz

RF

Ansoft HFSS 9.1

Fig. 38

5.87 GHz

3 MHz

19.4%

Fig. 39 CDRA

가 4~7GHz

가 가

VSWR 2

CDRA

가

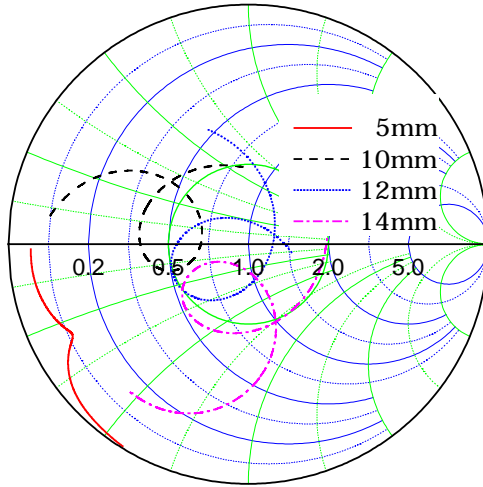


Fig. 39. Input impedance of a CDRA according to probe length



2.

CDRA

CDRA

CDRA

DRA

CDRA

Fig. 40

CDRA

가 l

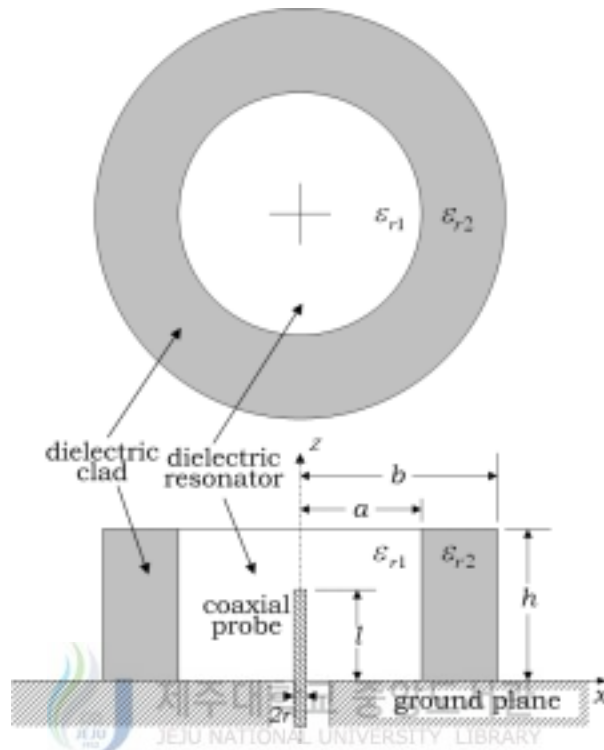


Fig. 40. Geometry of a CDRA with a dielectric clad

1) CDRA

가

Q

Fig. 40

$$\epsilon_{r1} = 10$$

$$a = 10.65\text{mm}$$

$$h = 10.6\text{mm}$$

CDRA

$$\epsilon_{r2} = 4$$

$$b/a \text{ 가 } 1.1$$

$$1.4$$

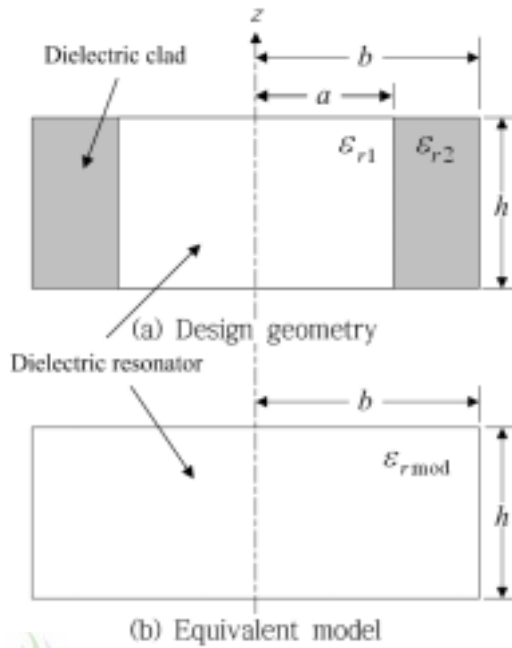
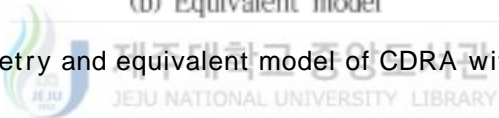


Fig. 41. Geometry and equivalent model of CDRA with dielectric clad



(43a) CDRA

$$f_u = 5.873 \text{ GHz}$$

$$\Delta f_u (BW) = 1.01 \text{ GHz}$$

가

. Fig. 41(a)

Fig. 41(b)

가

$$\epsilon_{r2}$$

$$\epsilon_{r1}$$

$$b/a$$

$$b/a = 1.1, 1.2, 1.3, 1.4$$

$$\epsilon_{r\text{mod}}$$

$$\epsilon_{r2} < \epsilon_{r\text{mod}} < \epsilon_{r1}$$

가

$$\varepsilon_{r\text{mod}} = \varepsilon_{r1} \times l_1 + \varepsilon_{r2} \times l_2 \quad (55)$$

$$l_1 = a/b \quad l_2 = (b-a)/b \quad .$$

$$b \quad h$$

$$3 \quad 1 \quad (44a), (44b) \quad (45)$$

Table 5

CDRA Table 5 가 (f_u, f_l)

$$(\Delta f_u, \Delta f_l) \quad (53)$$

Table 6

Table 5. Resonant frequency and bandwidth of equivalent model ($\varepsilon_{r2} = 4$)

h(mm)	b(mm)	$\varepsilon_{r\text{mod}}$	Resonant frequency f_l (GHz)	Bandwidth Δf_l (GHz)
10.6	1.72	9.46	5.57	0.597
	1.78	8.98	5.33	0.576
	13.84	8.62	5.08	0.564
	14.91	8.26	4.88	0.566

Table 6. Frequency response for each CDRA by eq. (53)

b/a	f_l	$(\Delta f_u + \Delta f_l)$ (GHz)	$2(f_u - f_l)$ (GHz)
1.1	5.57	$0.64 + 0.597 = 1.237$	0.6
1.2	5.33	$0.64 + 0.576 = 1.216$	1.08
1.3	5.08	$0.64 + 0.564 = 1.204$	1.58
1.4	4.88	$0.64 + 0.566 = 1.206$	1.98

Table 7. Frequency response for each CDRA by a simulation tool

b/a	f_l	$(\Delta f_u + \Delta f_l)$ (GHz)	$2(f_u - f_l)$ (GHz)	Frequency response
1.1	5.56	$1.01 + 1.04 = 2.05$	0.62	Broadband
1.2	5.22	$1.01 + 0.93 = 1.94$	1.30	Broadband
1.3	5.02	$1.01 + 0.84 = 1.85$	1.70	Broadband
1.4	4.79	$1.01 + 0.99 = 2.00$	2.16	dual - band

b/a 가 1.3 1.4

Fig. 34(b)

34(a)



Fig.

Table 6

RF

Table 7 HFSS

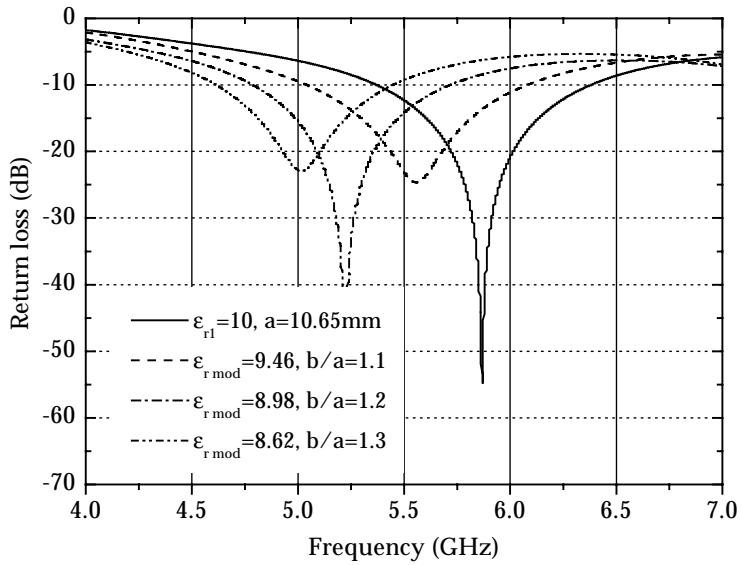
Table 6

b/a 가 1.4

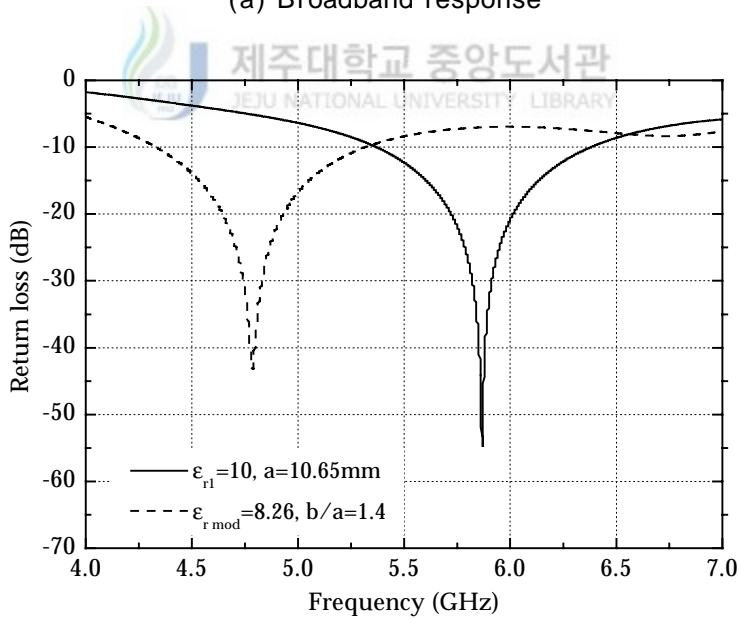
b/a 가 1.1, 1.2 1.3

Fig. 42

가



(a) Broadband response



(b) Dual - band response

Fig. 42. Return loss of equivalent model with according to b/a ratio

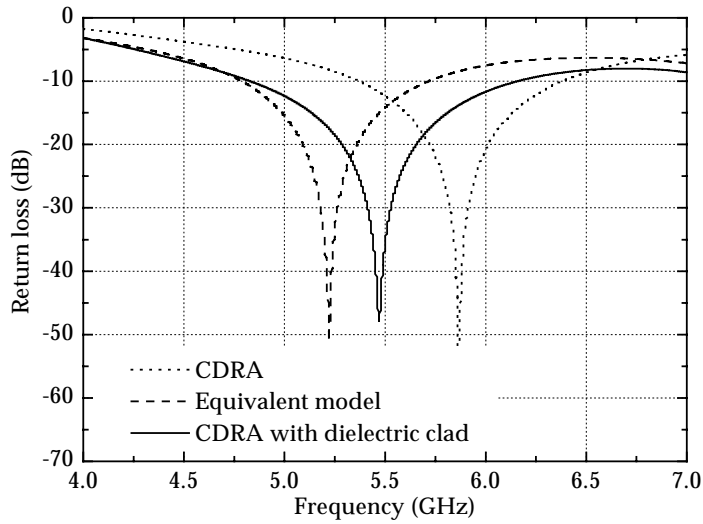


Fig. 43. Return loss of each CDRA ($b/a = 1.2$)

Fig. 42(a)



제주대학교 중앙도서관
JEJU NATIONAL UNIVERSITY LIBRARY

가 가
 b/a 가 1.1, 1.2 1.3 가

CDRA 10dB

. Fig.

42(b) CDRA b/a 가 1.4 가 10dB

가 $b = 11.72$ mm

$b = 13.85$ mm

가

CDRA 가

$b/a = 1.3$

Fig. 42

가

CDRA

$\epsilon_{r1} = 10$, $\epsilon_{r2} = 4$,

$a = 10.65$ mm,

$h = 10.6$ mm

$b/a = 1.2$

1.3

. Fig. 43 Fig. 44

b/a

1.2 1.3

CDRA, 가

CDRA

Fig. 43 $b/a=1.2$ CDRA 10dB 5.37~6.38 GHz
 CDRA 4.79~5.72 GHz 10dB
 CDRA 가 5.37~5.72GHz CDRA
 10dB 4.84~6.17 GHz , CDRA 10dB
 CDRA 10dB
 CDRA 24.3% 5.47 GHz
 $b/a=1.3$ Fig. 44 Table 8
 CDRA 10dB 5.37~6.38GHz 가 10dB
 4.61~5.45GHz
 5.37~5.45GHz CDRA 10dB
 4.52~6.35GHz CDRA 가

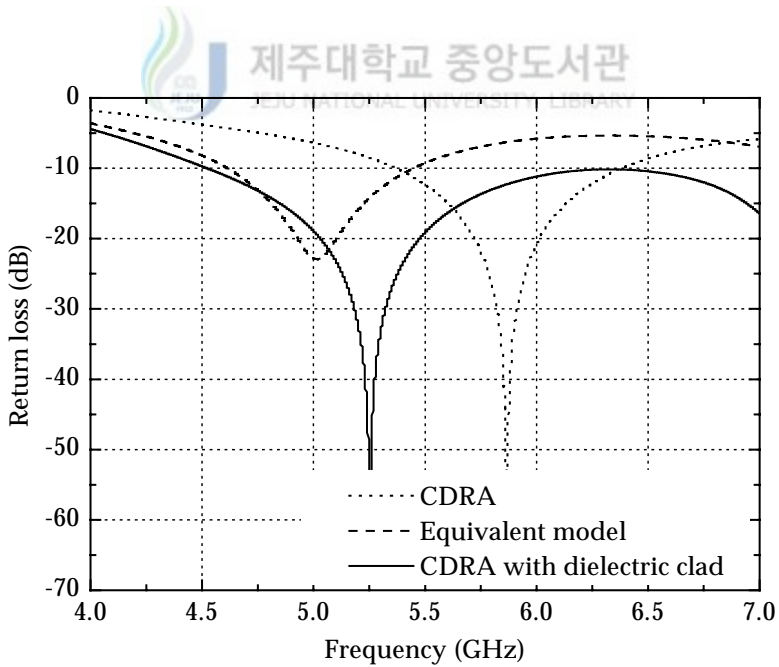


Fig. 44. Return loss of each CDRA ($b/a=1.3$)

Table 9

 $b/a = 1.3$

가

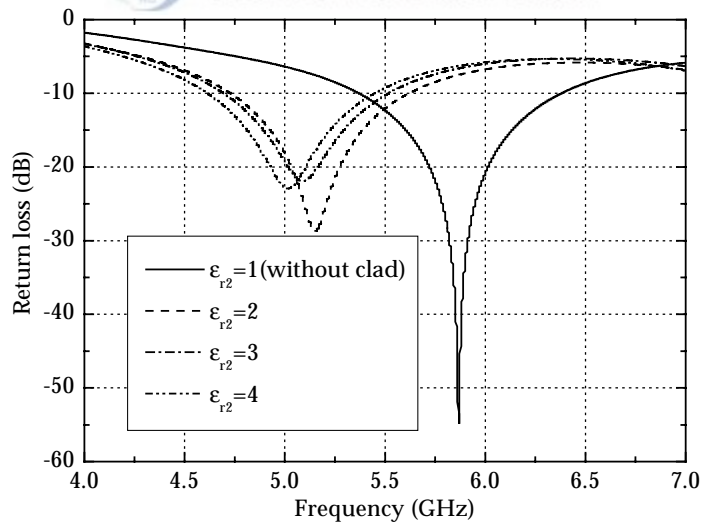
Fig. 44

Table 8. Comparison for each CDRA model($b/a = 1.3$)

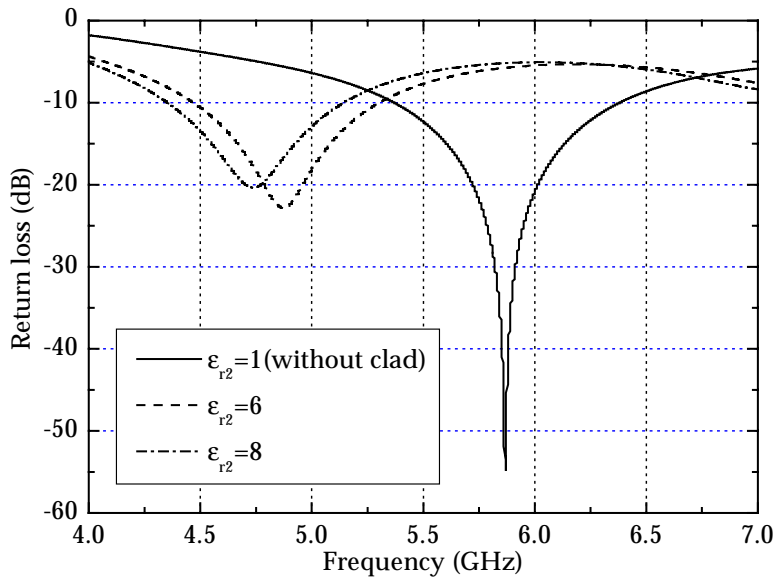
Model	Resonant Frequency (GHz)	Frequency range (GHz)	Relative Bandwidth (%)
CDRA	5.87	5.37 - 6.38	17.2
Equivalent model	5.0	4.61 - 5.45	16.8
CDRA with dielectric clad	5.25	4.52 - 6.35	34.8

Table 9. Design parameters of equivalent model with $b/a = 1.3$

ϵ_{r2}	2	3	4	6	8
$\epsilon_{r2\text{mod}}$	8.16	8.62	8.39	9.08	9.54



(a) Broadband response



(b) Dual - band response

Fig. 45. Return loss of equivalent model with $b/a=1.3$

Fig. 45

2, 3, 4

6, 8

Table 9 Fig. 45

$\epsilon_{r2} = 3$

CDRA 가

CDRA

Fig. 46

Fig. 46

CDRA 10dB

4.71~6.31 GHz , CDRA 10dB

(5.37~6.38 GHz) 가

10dB (4.69~5.52 GHz)

CDRA 29.5%

5.43 GHz

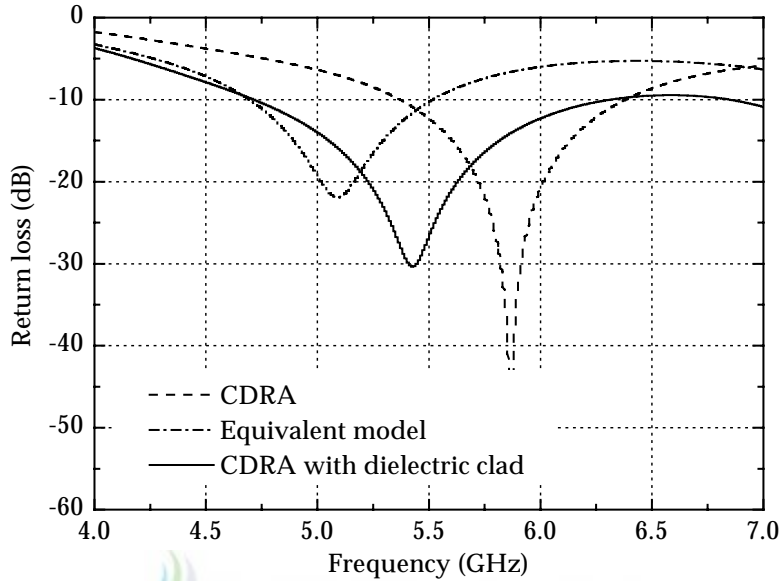


Fig. 46. Return loss of each CDRA

2) b/a

b/a

$\epsilon_{r2} = 3$

$\epsilon_{r1} = 10$, $a = 10.65$ mm,

$h = 10.6$ mm

b/a 1.1 1.5

l

Fig. 47 b/a

b/a 가 가

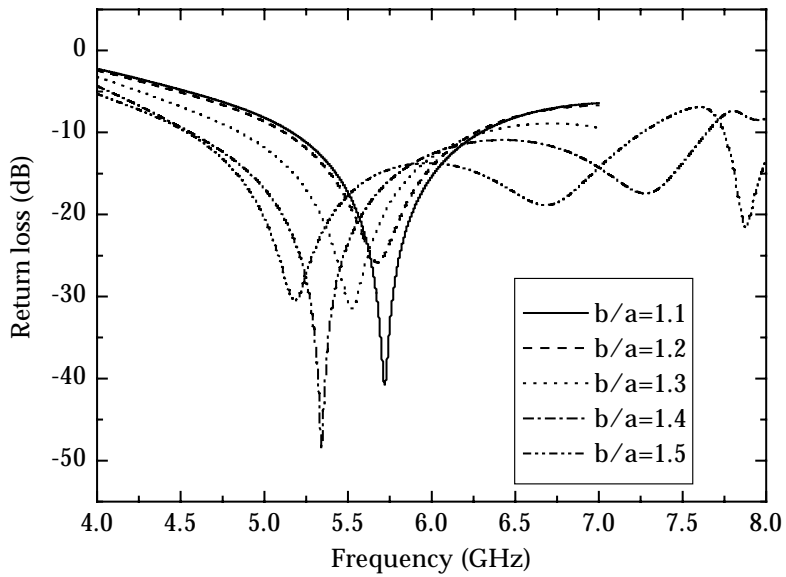


Fig. 47. Behavior of return loss with b/a as parameter

Table 10. Bandwidth and resonant frequency of CDRA with the dielectric clad according to b/a

b/a	Bandwidth (GHz)	Resonant frequency (GHz)
1.1	1.12	5.72
1.2	1.14	5.68
1.3	1.46	5.52
1.4	3.09	5.34
1.5	2.72	5.18

10dB

Table 10

b/a 가 1.4

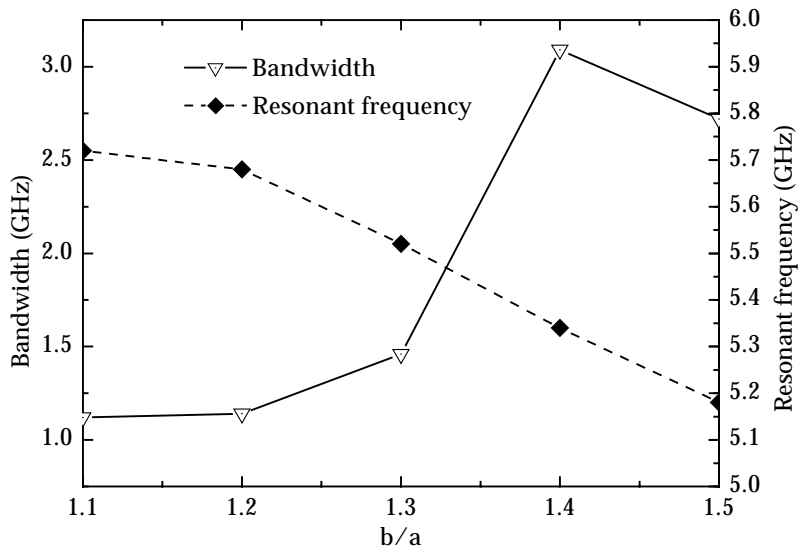


Fig. 48. Bandwidth and resonant frequency with b/a as parameter

Table 10



Fig. 48

b/a 가 가

가

가

가 1.4

5.72 GHz

5.18 GHz

10%

56%

Fig. 49 b/a

CDRA

3dBi

b/a

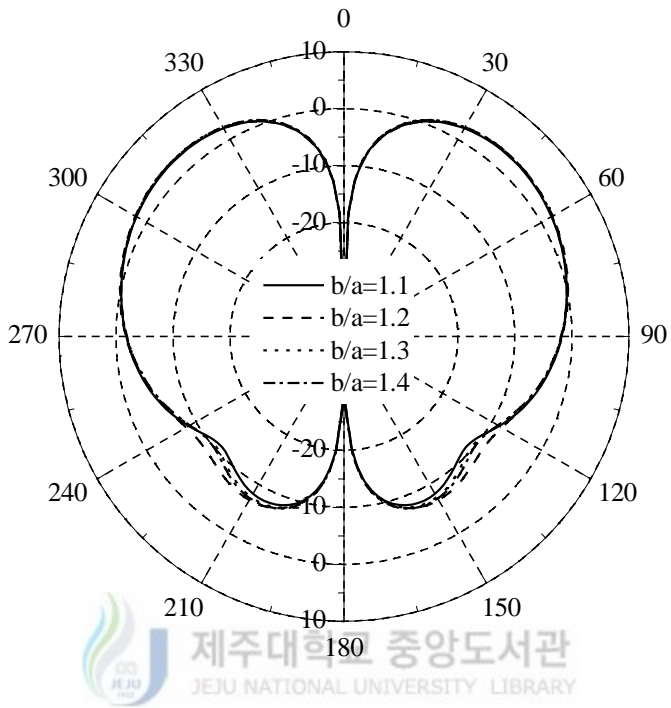


Fig. 49. Radiation patterns according to b/a

3)

$$\epsilon_{r1} = 10, \quad a = 10.65 \text{ mm}, \quad h = 10.6 \text{ mm} \quad b/a = 1.4$$

CDRA

1 6

가

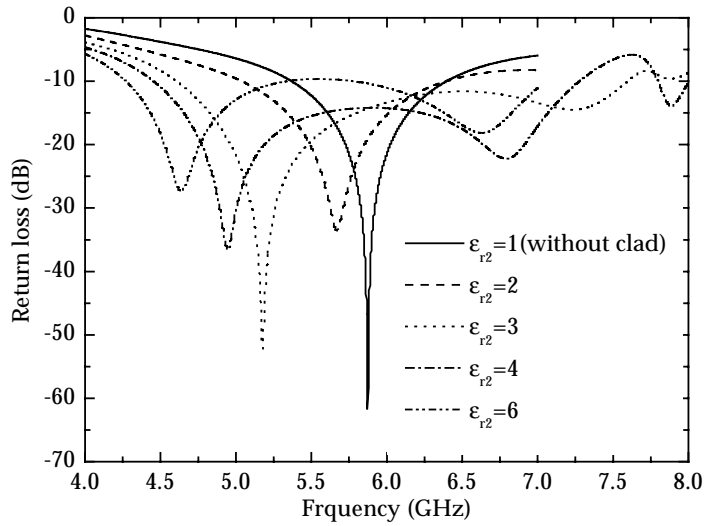


Fig. 50. Return loss of CDRA according to the relative permittivities of dielectric clad

Table 11. Resonant frequency and bandwidth according to ϵ_{r2} of dielectric clad

ϵ_{r2}	Resonant frequency (GHz)	Bandwidth (MHz)
2	5.67	5.04~6.39
3	5.18	4.61~7.59
3.3	5.14	4.61~7.71
4	4.94	4.45~7.28
6	4.64	4.27~5.34

Fig. 50

가

Table 11

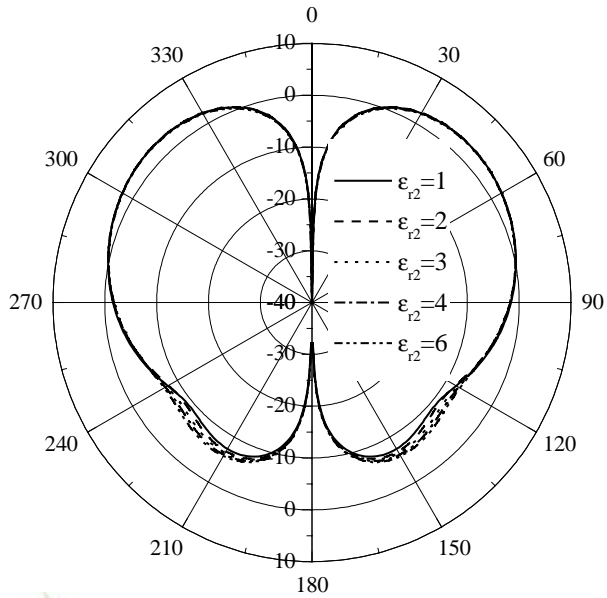


Fig. 52. Radiation patterns according to the relative permittivities of dielectric clad

b/a

가

4)

CDRA

CDRA

$\epsilon_{r1} = 36$

CDRA

$a = 10.65 \text{ mm}, h = 10.6 \text{ mm}$

$f_u = 3.095 \text{ GHz}$

$\Delta f_u = 0.035 \text{ GHz}$

DRA

1/3

$\epsilon_{r2} = 12$

가 (55)

$$b \quad h \quad (44a), (44b) \quad (45)$$

Table 12

Table 12

HFSS

Fig. 53

Table 12. Frequency response for each CDRA's

b/a	f_l	$(\Delta f_u + \Delta f_l)$	$2(f_u - f_l)$
1.1	2.97	$0.035 + 0.037 = 0.0720$	0.25
1.2	2.85	$0.035 + 0.0319 = 0.066$	0.49
1.3	2.75	$0.035 + 0.0404 = 0.075$	0.69
1.4	2.65	$0.035 + 0.0435 = 0.078$	0.89

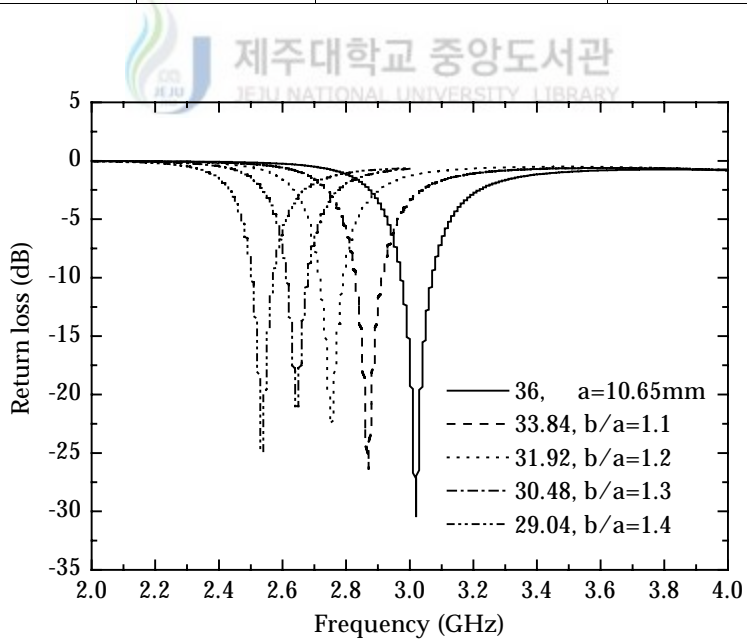


Fig. 53. Return loss of CDRA according to modified relative permittivities

Table 12

$$\epsilon_{r1} = 36$$

10dB

. Fig. 53

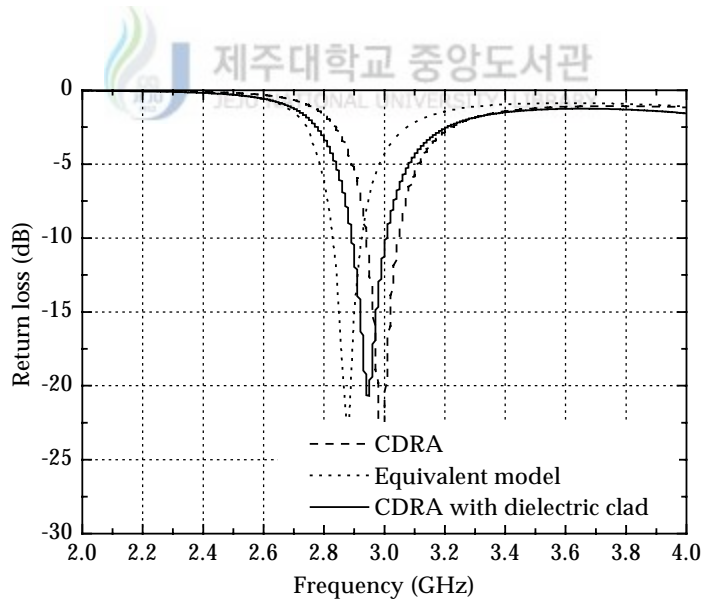
Table 13

$$b/a = 1.1$$

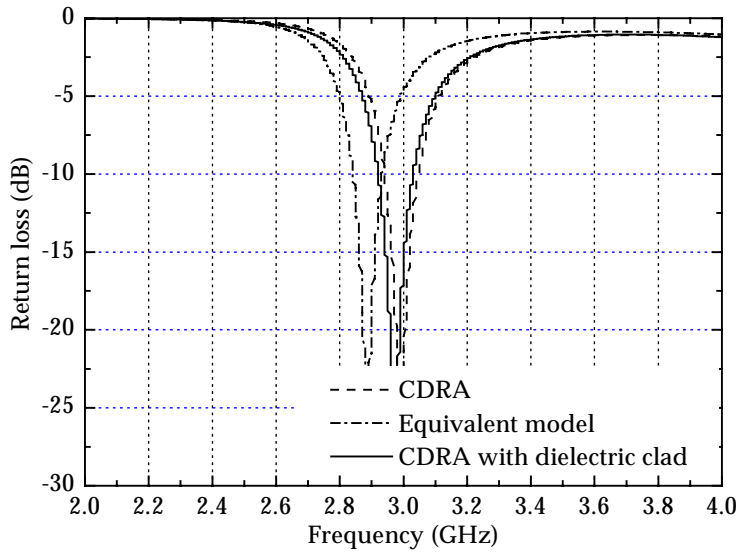
$$\epsilon_{r2} = 2, 4$$

Table 13. Design parameters of CDRA with dielectric clad

	ϵ_{r1}	ϵ_{r2}	h(mm)	a(mm)	b/a
Model 1	36	2	10.6	10.65	1.1
Model 2	36	4			



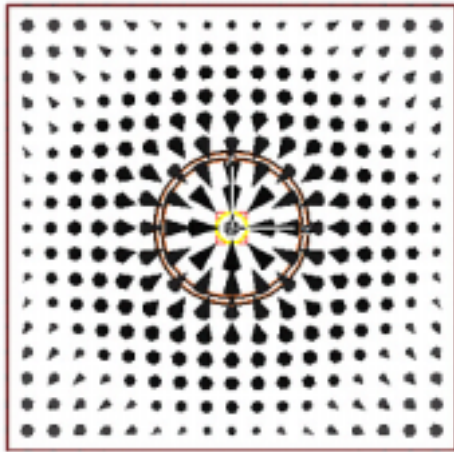
(a) Model 1 ($\epsilon_{r2} = 2$)



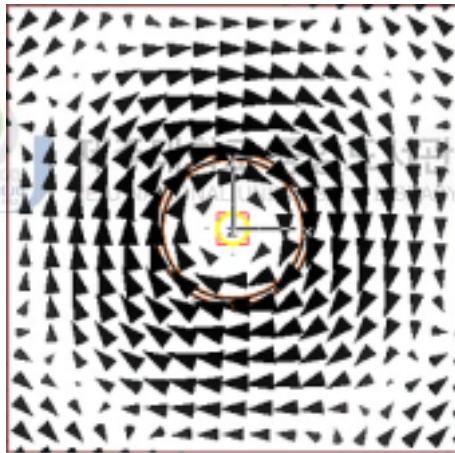
(b) Model 2 ($\epsilon_{r2} = 4$)

Fig. 54. Return loss for three CDRA models

Table	13	CDRA	가	$\epsilon_{r2} = 2$
		CDRA	Fig. 54	Fig. 54
		CDRA	3.6%	CDRA
	4.1%가	$\epsilon_{r2} = 4$		CDRA
	3.9%	CDRA		
		가		
	CDRA			
	b/a	1.4		
		1/3		



(a) E - field



(b) H - field

Fig. 55. Field distribution of the CDRA with dielectric clad

Fig. 40

$TM_{01\delta}$

Fig. 55

CDRA

5)

CDRA

CDRA

Fig. 56

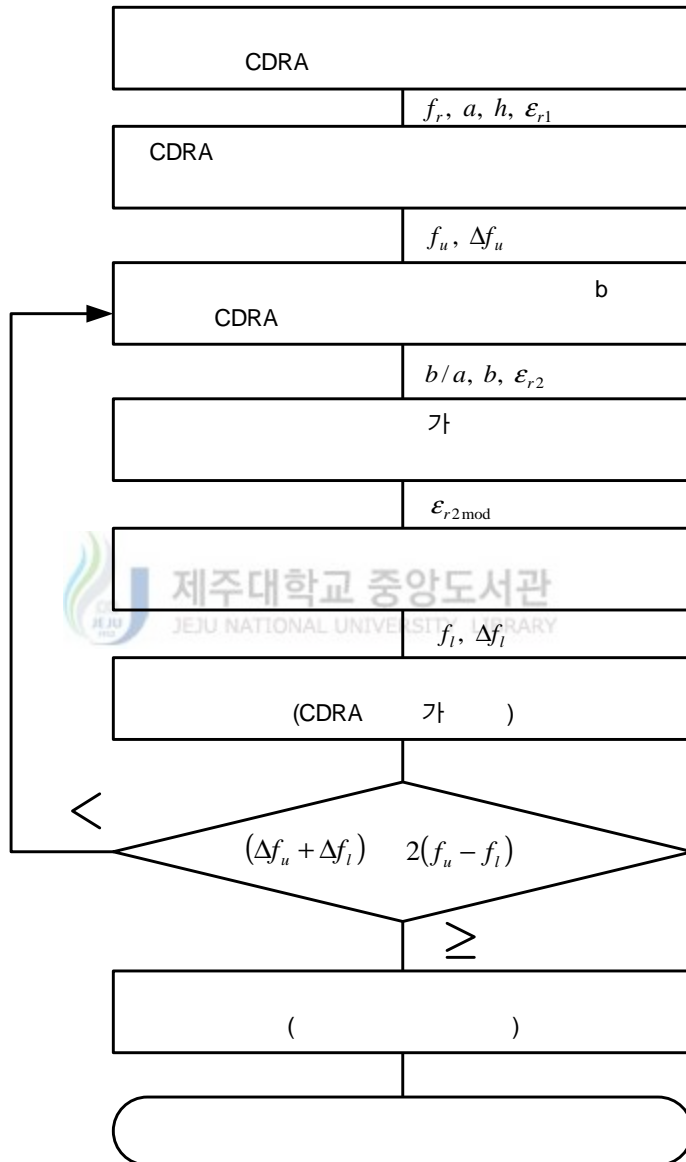


Fig. 56. Flow chart for design procedure

CDRA

Q

Fig. 56



V.

1.

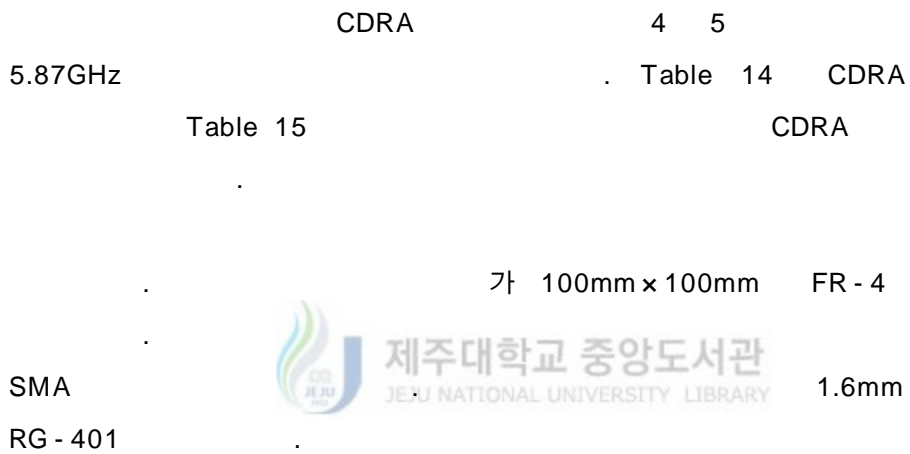
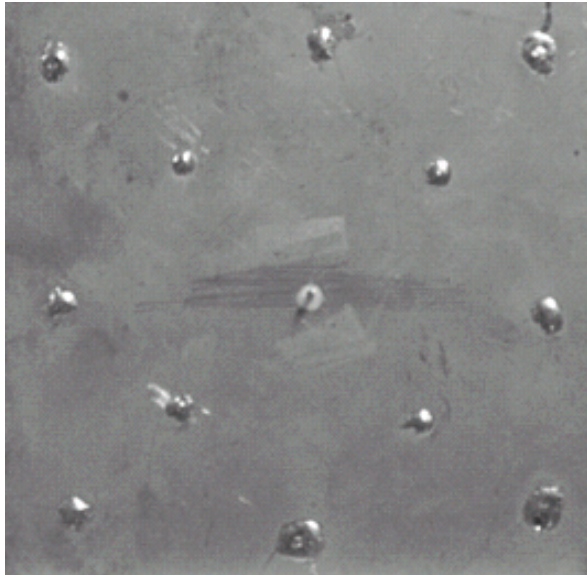


Table 14. Fabricated parameters of CDRA

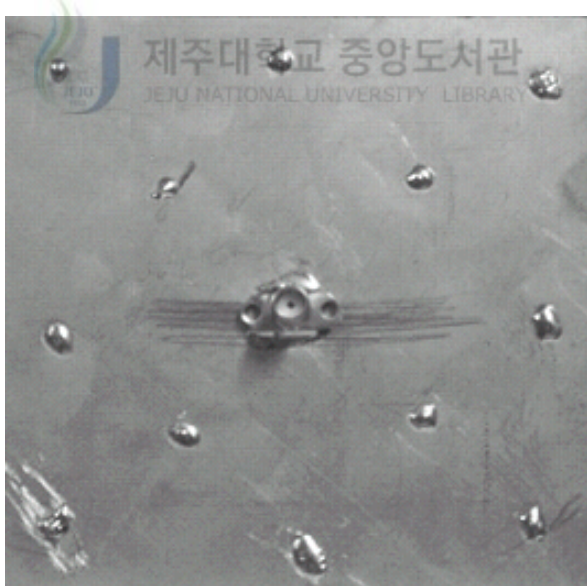
ϵ_{r1}	Radius a(mm)	Height h(mm)
10	10.65	10.6

Table 15. Fabricated parameters of CDRA with dielectric clad

ϵ_{r1}	ϵ_{r2}	a(mm)	b(mm)	h(mm)	b/a
10	4	10.65	15.35	10.6	1.44



(a) Front view



(b) Back view

Fig. 57. Photos of coaxial probe feed

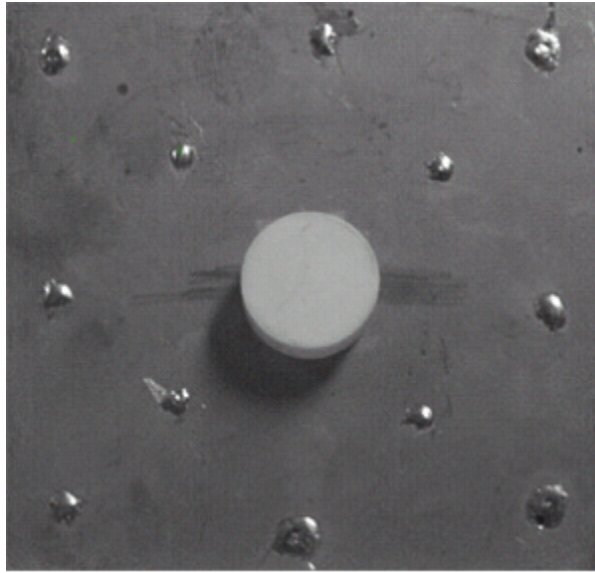


Fig. 58. Photo of the fabricated CDRA



Fig. 57

Fig. 58

$\epsilon_r = 10$, $a = 10.65mm$,
 $h = 10.6mm$.
 $TM_{01\delta}$ 가

Fig. 59 Table 15

가

CDRA

Fig. 57

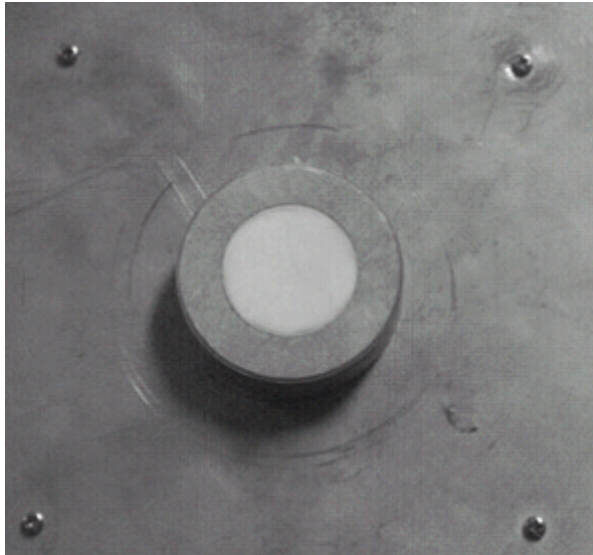


Fig. 59. Photo of the fabricated CDRA with dielectric clad



2.

1)

GHz	17.3%	5.94 GHz	Fig. 60
61	CDRA	CDRA	5.87~6.9
	E_θ	E_ϕ	Fig.
		$\lambda/4$	
		55°	
3.2dB			

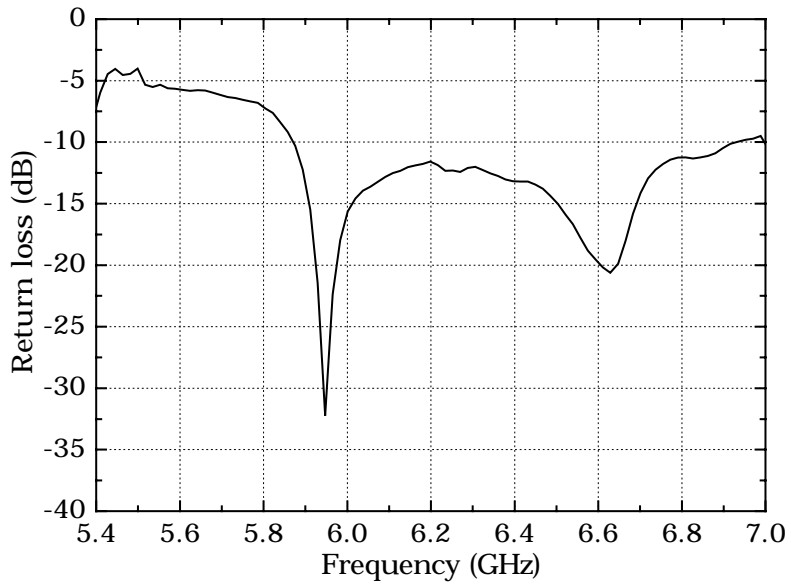


Fig. 60. Measured return loss of CDRA

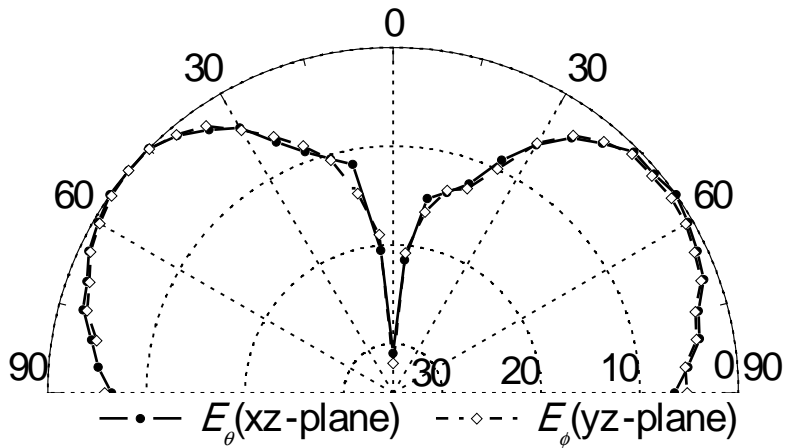


Fig. 61. Measured radiation patterns of CDRA

2)

DRA

Fig. 62

Table 16

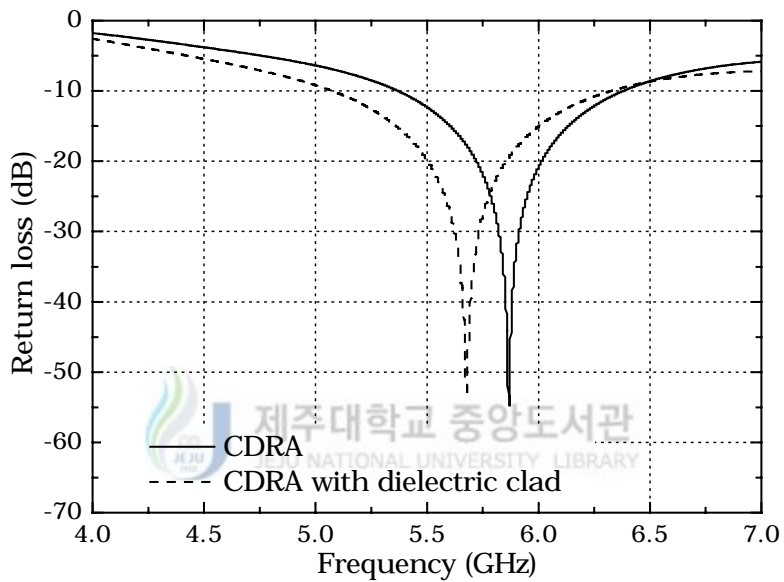


Fig. 62. Return loss of CDRA and CDRA with dielectric clad

Table 16. Resonant frequency and relative bandwidth for each models

	Resonant Frequency (GHz)	Frequency Range (GHz)	Relative Bandwidth (%)
CDRA	5.87	5.37 ~ 6.38	17.2
CDRA with dielectric clad	5.68	5.07 ~ 6.32	22.2

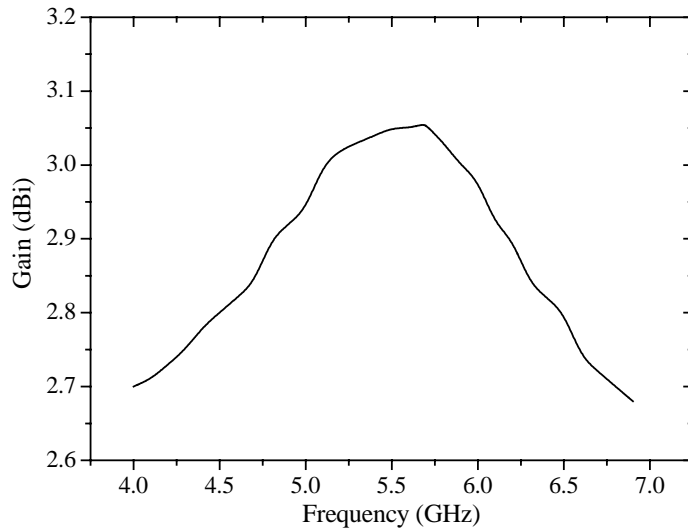


Fig. 63. Gain of the fabricated CDRA with dielectric clad

Fig. 63



CDRA
3.1 dBi
가 5.07 GHz
6.32 GHz 2.7dBi 3.1dBi

Fig. 64 CDRA

CDRA 1.03 GHz 5.94 GHz CDRA
1.7 GHz 5.91 GHz CDRA CDRA
17.3%, 28.8% 11.5% . Fig. 65

CDRA

CDRA

50°

3dBi가

CDRA

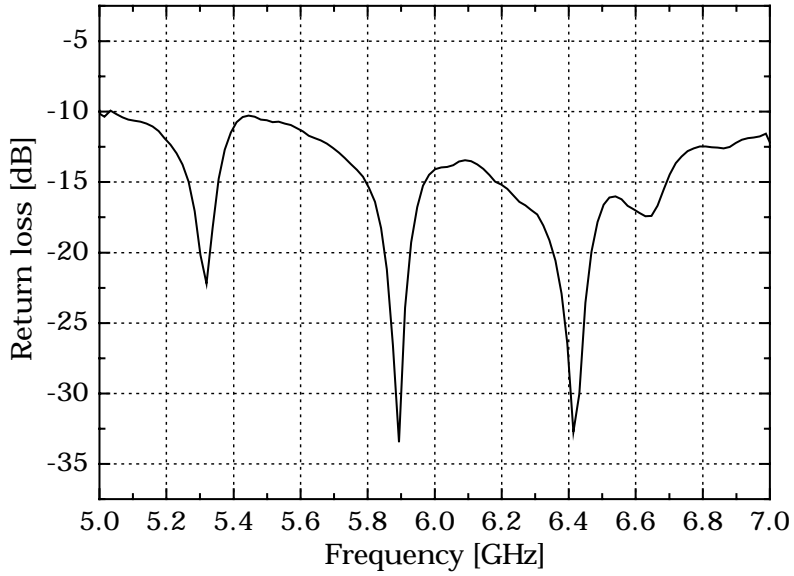


Fig. 64. Return loss of the fabricated CDRA with dielectric clad

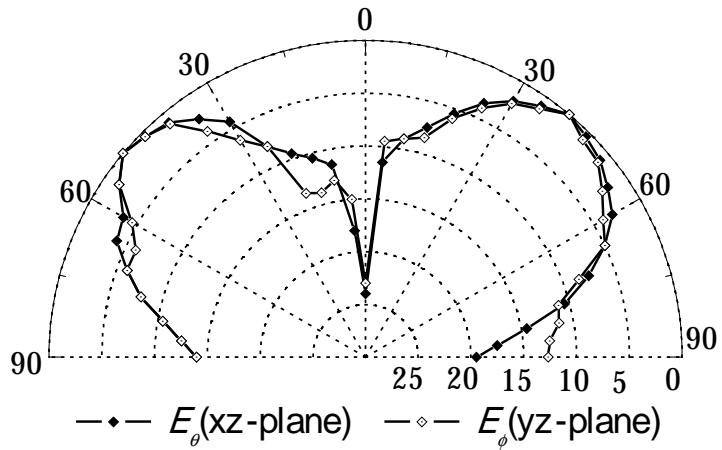


Fig. 65. Measured radiation patterns of CDRA with dielectric clad

CDRA
Embedded DRA가 . DRA
DRA
Q
가
가
Table 3
5.63GHz 8.64GHz 가 .
CDRA가 DRA
21% .
가
38% . 가
CDRA가 DRA



CDRA

CDRA

가

가 1.3

1.2



3
제주대학교 중앙도서관
JEJU NATIONAL UNIVERSITY LIBRARY

(FEM) HFSS

가 가

가 1.4

1/3

40%

$\epsilon_{r1} = 10$, $a = 10.65$ mm, $b/a = 1.44$ $\epsilon_{r2} = 4$

가 5.68GHz

22.2%

가 5.91GHz

28.8%

4%

$\epsilon_{r2} = 3.3$ $b/a = 1.4$

22% DRA 60%
38% CDRA가 DRA

가

가



- Bladel, J.V. and Verplanken, M., 1976, The electric - dipole resonances of ring resonators of very high permittivity, *IEEE Trans. on Microwave Theory & Tech.*, pp. 108~111.
- Chen, N.C., Wong, K.L., 1995, Input impedance of a slot - coupled multilayered hemispherical dielectric resonator antenna, *IEEE Int. Antennas Propagat. Symp. Dig.* vol. 33, pp.1796~1799.
- Chow, K.Y., Leung, K.W., Luk, K.M. and Yung, E.K.N., 1997, Cylindrical ring dielectric resonator antenna excited by a soldered - through probe, *Asia Pacific Microwave Conference*, pp.625~628.
- Fan, Z. and Antar, Y.M.M., 1997, Slot - coupled DR antenna for dual - frequency Operation, *IEEE Trans. on Antennas & Propagation*, Vol. 45, No. 2, pp.306~308.
- Junker, G.P., Kishk, A.A., Glisson, A.W. and Kajfez, D. 1994, Effect of air gap on cylindrical dielectric resonator antenna operating in $TM_{01\delta}$ mode, *IEE Electronics Letters*, Vol. 30, no. 2, pp.97~98.
- Junker, G.P., Kishk, A.A., Glisson, A.W. and Kajfez, D. 1995, Effect of fabrication imperfections for ground plane - backed dielectric - resonator antennas, *IEEE Antennas & Propagation Magazine*, Vol. 37, no. 1, pp.40 - 45.
- Kajfez, D. and Guillon, P., 1986, Dielectric resonator, Artech house, pp.72~82.
- Kajfez, D., Kishk, A.A. and Ahn, B., 1989, Broadband stacked dielectric resonator antennas, *IEE Electronics Letters*, Vol. 25, No. 18, pp.1232 - 1233.
- Kishk , A.A. and Glisson, A.W., 2001, Bandwidth enhancement for split cylindrical

- dielectric resonator antennas, *Progress In Electromagnetic Research, PIER*, 33, pp.97~118.
- Kishk, A.A., Ittipiboon, A., Antar, Y.M.M. and Cuhaci, M., 1985, Slot excitation of the dielectric disk radiator, *IEEE Trans. on Antennas & Propagation*, Vol. 43, No. 2, pp.198 - 201.
 - Kranenburg, R.A., Long, S.A. and Williams, J.T., 1990, Coplanar waveguide excitation of dielectric resonator antennas, *IEEE Trans. on Antennas & Propagation*, Vol. 39, No. 1, pp.119~122.
 - , , 2001, “ LAN ” , , Vol. 12, No. 3, pp.425~431.
 - , , 2003, “ ” , , Vol.40. No.4, pp.54~57.
 - Lee, M.T., Luk, K.M., Leung, K.W. and Yung, E.K.N., 1999, Novel feeding technique for dielectric resonator antennas, *IEEE Int. Antennas Propagat. Symp. Dig.* Vol. 37, pp. 92~95.
 - Lee, M.T., Luk, K.M., Leung, K.W. and Leung, M.K., 2002, A small dielectric resonator antenna, *IEEE Trans. on Antennas & Propagation*, Vol. 50, No. 10, pp.1485~1487.
 - Leung, K.W., Chow, K.Y., Luk, K.M. and Yung, E.K.N., 1996, Offset dual - disk dielectric resonator antenna of very high permittivity, *IEE Electronics Letters*, Vol. 32, No. 22, pp.2038~2039.
 - Leung, K.W., Chow, K.M., Luk, K.M. and Yung, E.K.N., 1997, Low - profile circular disk DR antenna of very high permittivity excited by a microstripline, *IEE Electronics Letters*, Vol. 33, No. 12, pp.1004~1005.
 - Leung, K.W., Wong, W.C., Luk, K.M. and Yung, E.K.N., 1998, Annular slot - coupled dielectric resonator antenna, *IEE Electronics Letters*, Vol. 34, No. 13, pp.1275~1276.

- Leung, K.W., Chen, Z.N., Luk, K.M. and Yung, E.K.N., 1999, On the aperture - coupled dielectric resonator antenna using a thick ground plane, *IEEE Int. Antennas Propagat. Symp. Dig.* vol. 37, pp.2792~2795.
- Lo, H.Y., Leung. K.W., Luk, K.M. and Yung, E.K.N., 2000, Low profile triangular dielectric resonator antenna, *IEEE Int. Antennas Propagat. Symp. Dig.* Vol. 38, pp. 2088~2091.
- Long, S.A., Mcallister, M.W. and Sheen, C., 1983, The resonant cylindrical dielectric cavity antenna, *IEEE Trans. on Antennas & Propagation.*, Vol. 31, No. 3, pp.406 - 412.
- Luk, K.M. and Shum, S.M., 1994, Bandwidth enhancement of probe - fed dielectric ring resonator antenna with parasitic element, *IEEE Int. Antennas Propagat. Symp. Dig.* vol. 32, pp.768~771.
- Luk, K.M. and Leung, K.W., 2003, Dielectric resonator antenna, Research studies press, pp.1~211.
- Martin, J.T.H.ST., Antar, Y.M.M., Kishk, A.A., Ittipiboon, A. and Cuhaci, M., 1990, Dielectric resonator antenna using aperture coupling, *IEE Electronics Letters*, Vol. 26, No. 24, PP.2015~2016.
- Mongia, R.K., Ittipiboon, A., Bhartia, P. and Cuhaci, M., 1993, Electric monopole antenna using a dielectric ring resonator, *IEE Electronics Letters*, Vol. 29, No. 17, pp. 1530 - 1531.
- Mongia, R.K. and Ittipiboon, A., 1997, Theoretical and Experimental investigations on rectangular dielectric resonator antenna, *IEEE Trans. on Antennas & Propagation*, vol.45, no.9, pp.1348 - 1356.
- Nannini, C., Ribero, J.M., Dauvignac, J.Y. and Pichot, Ch., 2004, Bifrequency behaviour and bandwidth enhancement of a dielectric resonator antenna, *Microw. & Opt. Technol. Lett.*, Vol. 42, No.5, pp. 432~434.

- Ong, S.H., Kishk, A.A. and Glisson, A.W., 2002, wideband disk ring dielectric resonator antenna, *Microwave & Optical Tech. Letters*, Vol. 35, No. 6, pp.425~428.
- Petoas, A., Ittipiboon, A., Antar, Y.M.M., Roscoe, D. and Cuhaci, M., 1998, Recent advances in dielectric resonator antennas, *IEEE Antennas & Propagation Magazine*, Vol. 40, no. 3, pp.35~48.
- Sangiovanni, A., Dauvignac, J.Y. and Pichot, C., 1997, Embedded dielectric resonator antenna for bandwidth enhancement, *IEE Electronics Letters*, Vol. 33, No. 35, pp. 2090~2091.
- Shum, S.M. and Luk, K.M., 1994, Characteristics of dielectric ring resonator antenna with an air gap, *IEE Electronics Letters*, Vol. 30, No. 4, pp.277 - 278.
- Shum, S.M. and Luk, K.M., 1995, Stacked annular ring dielectric resonator antenna excited by axi - symmetric coaxial probe, *IEEE Trans. on Antennas and Propagation*, Vol. 43, no. 8, pp.889~892.



가



89

, R.O.T.C 19

가